University of Alberta

Fabrication and characterization of PZT nanorods and nanohexagons with applications in piezoelectric transducers

by

Qian Wan

A thesis submitted to the Faculty of Graduate Studies and Research
in partial fulfillment of the requirements for the degree of

Master of Science
in
Microsystems and Nanodevices

Department of Electrical and Computer Engineering

Fall 2012
Edmonton, Alberta

Abstract

All ultrasound devices/sensors use piezoelectric transducers to generate/receive ultrasound. These transducers are made of Pb ($Zr_{0.53}Ti_{0.47}$) O_3 (PZT) materials. In this article, we report a new way of fabricating PZT material with interesting nanorod and nanohexagon shapes. The PZT nanohexagons with typical diameters and bounding lengths within the nanometer range were synthesized by sintering a mixture of PZT nanocrystals, Tween 20 and sodium chloride, in which the PZT nanocrystals were made by a sol-gel method. The PZT nanorods were also synthesized by sintering a mixture of PZT nanocrystals, Triton and sodium chloride. After annealing at 800°C for three hours, PZT nanorods and PZT nanohexagons formed and exhibited a single-crystalline nanostructure, confirmed by high resolution transmission electronic microscopy (HRTEM). X-ray diffraction (XRD) and Raman Spectra studies demonstrated their crystal structures and composition, scanning electron microscopy (SEM) and transmission electron microscopy (TEM) were used to image their morphologies.

Acknowledgement

I would like to acknowledge Dr. Jie Chen for his supervision during my Master study. It is him who gives me the opportunity to pursue my Master in this world-class university. Furthermore, it is also him that provides me with a harmonious, comfortable and freedom research environment, so that I am able to concentrate on my study and research projects. In addition, it is him that brings me in and always guides me in the research world. In all, I would like to give my deep gratitude and respect to him first.

This cross-disciplinary research has been stimulating and challenging, and the most importantly, it gives me a chance to use my innovation, which will impact my career development. I would like to extend my appreciation to the members of my thesis committee – Dr. Hao Zhang and Dr. Jie Han, for their guidance and advice.

I would also like to acknowledge Dr. Quanrong Gu for his patient instruction and valuable inputs. It is him that brought me into the fascinating world of my thesis research. Dr. Gu also taught me research techniques. Therefore, I would like to give my deep gratitude and respect to him as well.

I would also like to acknowledge Dr. James Xing for his valuable suggestions and vast knowledge for our projects. I would also like to thank him for his cooperation

with Dr. Jie Chen to bring us financial support and lab equipments to accomplish our research projects.

At the end, I would like to thank Dr. Jian Chen and Hui Qian from the National Institute for Nanotechnology (NINT), National Research Council Canada for their valuable inputs and generous help in my research projects. I would also like to acknowledge the funding supports from NSERC discovery and NSEC collaborative research and development program.

Table of Contents

List of Tables

List of Figures

Chapter 1 Introduction

1.1 Background on PZT

Lead zirconium titanate ($Pb[Zr_xTi_{1-x}]O_3$, $0 \leq x \leq 1$) or PZT as an abbreviation, is a ceramic perovskite material with a remarkable piezoelectric effect. Basically, the PZT-based compounds are composed of the chemical elements: lead and zirconium, and the chemical compound titanate. They are used in the manufacturing of piezoelectric transducers or ultrasound sensors. The compounds are combined under extremely high temperatures, followed by a mechanical filter to filter out the particulates. With the wide use of PZT transducers, we are looking into how to make the transducer cheaper with the state-of-the-art nano-fabrication technology. A transducer is a device that converts energy from electronic signals to mechanical vibrations. Since piezoelectric devices use a very reliable and inexpensive way to convert electrical energy into physical motions and it exhibits high tolerance to environmental factors such as electromagnetic fields and humidity, piezoelectric material has been widely used as a basic component of transducers.

A vibrating piece is included in a piezoelectric transducer which has on both of its surfaces electrodes to provide an electric field to the vibrating piece. More specifically, the electric signals are converted into mechanical vibrations or vice versa by using the morphological change of a crystal that occurs on voltage

application, or inversely by monitoring the voltage generated by a pressure applied on a crystal. Commonly, piezoelectric transducers employ a ceramic piezoelectric element with electrodes on its oppositely polarised surfaces. As we know, piezoelectric transducers have many applications. Particularly, piezoelectric diaphragms have been regarded as pressure sensors, in speakers for audio equipment, fluid pumping and printing applications. A temporary potential difference across the electrodes is produced by a change of stress in the piezoelectric element. Due to these characteristics, a piezoelectric element is able to act as both a sensing and a transmitting element. Figure 1.1[1] displays a ceramic PZT. A piezoelectric element, however, is a crystal which delivers a voltage and deforms mechanically when a mechanical force is applied between its faces. The driver charges and discharges the piezoelectric disc rapidly, leading to high impedance state in preparation automatically to receive an echo. Piezoelectric transducers have been traditionally used to convert electric signals to mechanical vibrations, for instance: sound waves.

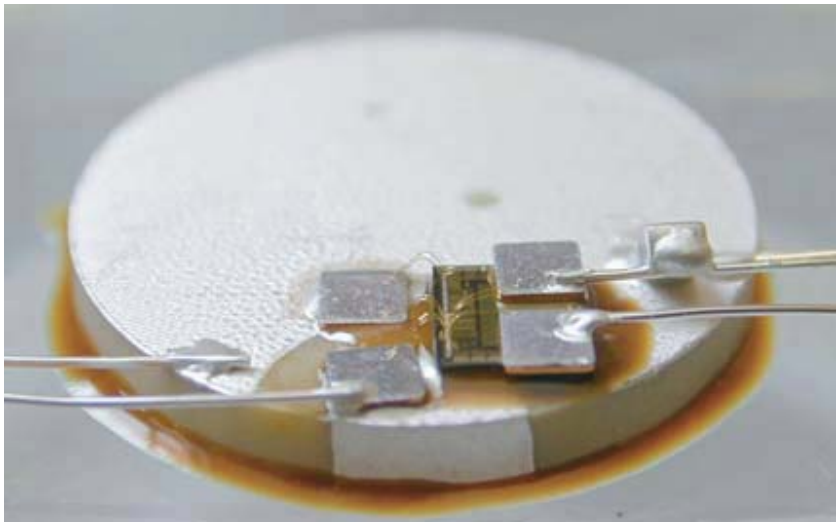

Figure 1.1 Ceramic PZT [1]

1.2 Piezoelectricity

Piezoelectricity is directly resulted from the piezoelectric effect, which is understood as the linear electromechanical interaction between the mechanical and the electrical state in crystalline materials with no inversion symmetry [2]. The word piezoelectricity means electricity coming out from pressure. It is originated from the Greek piezo or piezein, which means to squeeze or press, and electric or electron, which stands for amber, an ancient source of electric charge [3]. The piezoelectric effect is a reversible process in the materials exhibiting the direct piezoelectric effect (the internal generation of electrical charge resulting from an applied mechanical force) and also exhibiting the inverse piezoelectric effect (the internal generation of a mechanical force resulting from an applied electrical field). For instance, lead zirconium titanate crystals will generate measurable piezoelectricity when their static structure is deformed. Inversely, the same crystals will change their static dimension when applying an external electric field to the material.

Piezoelectricity is a phenomenon, when subjected to mechanical pressure, positive and negative electric charges appear simultaneously on opposite sides of some non-conducting crystals. It is the charge which accumulates in certain solid materials, for instance: notably crystals, certain ceramics, and biological matter such as bone, DNA and various proteins [4] in response to applied mechanical strain. The reason why piezoelectricity exists is that some atomic lattice structures

have an essential cell a cubic or rhomboid atomic cage, and this cage holds a semi-mobile ion which has several steady quantum position states inside itself. On the other hand, the converse piezoelectric effect - electrostriction is the property of some non-conductors or dielectrics which deform slightly under the application of an electric field.

Presently, piezoelectricity is the basis of a lot of scientific instrumental techniques with atomic resolution, the scanning probe microscopies, for example: STM, AFM, MTA, SNOM and so on. Furthermore, it is also found in lots of useful applications such as the production and sound detection, high voltages generating, generation of electronic frequency, microbalances, and ultrafine focusing of optical assemblies. Some daily uses such as the push-start propane barbecues and the ignition source for cigarette lighters.

1.3 Mechanism

The mechanism of the piezoelectric effect is closely related to the occurrence of electric dipole moments in solids, which may either be induced for ions on crystal lattice sites with asymmetric charge surroundings or may directly be carried by molecular groups. In general, dipoles near each other tend to be aligned in regions called Weiss domains, which are usually oriented randomly, but can be aligned using the process of polarization (a strong electric field is applied across the material, usually at elevated temperatures). However, not all piezoelectric materials can be polarized. Since each dipole is a vector, the dipole density P is also a vector or a directional quantity. The dipole density or polarization can easily be calculated

for crystals by adding up the dipole moments per volume of the crystallographic unit cell.

The decisive importance for the piezoelectric effect is the changing of polarization P when a mechanical stress is applied, which may be caused by either a re-configuration of the dipole-inducing surrounding or a re-orientation of molecular dipole moments under the influence of the external stress. Piezoelectricity is caused by dipole density in the bulk, but not by a change in charge density on the surface. Piezoelectricity may occur when there is a variation of the polarization strength or direction, or both of them, with the details depending on (1) the orientation of P in the crystal, (2) crystal symmetry, (3) the applied mechanical stress. Since the units of polarization and surface charge density are the same, the change in P appears as a variation of surface charge density upon the crystal faces (as a variation of the electrical field extending between the faces). Figure 1.2 illustrates that a voltage is generated when a piezoelectric disk is deformed.

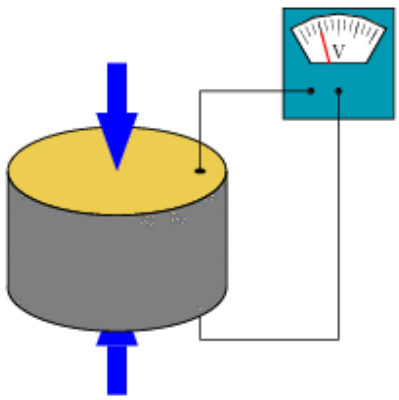

Figure 1.2 A piezoelectric disk generates a voltage when deformed [5]

1.4 Thesis objectives

PZTs are prototypical piezoelectric materials, which are able to convert mechanical vibrations to electric signals or vice versa. They are broadly used in actuators, sensors and transducers. PZTs are also perfect materials used in micro electromechanical systems (MEMS) and nano electromechanical systems (NEMS) due to their outstanding piezoelectric property, thus great efforts have been made to the synthesis of PZT microstructures and nanostructures. The properties of PZT nanocrystals depend on many factors such as shape morphology, size distribution and chemical composition, etc. Therefore, a general method for producing well-crystallized nanostructures would be of great interest. Investigations on these issues will be reported in the remaining chapters of this thesis.

Since the piezoelectric properties of the PZT materials with different morphologies vary from one to the other, the shape control of the PZT material has been a heated issue in the research area. Despite intensive experimental efforts have been made, the shape control of single-crystalline nanostructure has been difficult to achieve and turns out to be a challenge. It is the author's belief that the sizes and morphologies of the nanocryatals could be controlled by carefully selecting of the kind of surfactant and its concentration. In this thesis, an inorganic salt-surfactant-assisted method is proposed to the synthesis of single-crystalline PZT nanorod and nanohexagon. Experiments to understand the growth mechanism of the nanohexagons have been taken and detailed models for growth mechanism

have been proposed. In order to synthesize PZT nanostructures with different morphologies, a two-step synthesis method is presented in this project. The steps are described as follows:

1. Synthesis of PZT nanocrystals;

2. Synthesis of PZT nanostructures with different shapes by mixing the prepared PZT nanocrystals with NaCl and surfactants.

1.5 Outline

Chapter 2 gives us a general idea of the approaches which can be used to fabricate PZT crystals with a composition of $Pb(Zr_{0.52}Ti_{0.48})O_3$. Conventional method, hydrothermal method and sol-gel method are introduced in this chapter, and the reasons why sol-gel method is proposed in this project are also given. Chapter 3 illustrates the way of solution preparation and solvent selection. Detailed steps of producing and characterizing PZT nanocrystals are shown in this chapter. Chapter 4 is divided into two major parts. In part one, the properties of various types of synthesis approaches are studied and analyzed to identify a suitable candidate for this project. A salt-surfactant-assisted method is proposed in this project and the selection of surfactants is also described. The remainder of the chapter is dedicated to fabrication and characterization of the PZT nanostructures with different morphologies. More specifically, two different shapes of PZT nanostructures have been produced and displayed: PZT nanorods and PZT nanohexagons. The successful fabrication of PZT nanorods and PZT nanohexagons are confirmed using X-ray diffraction, Raman Spectra and Transmission Electron Microscopy. In

Chapter 5, the necessity of the surfactant is discussed and the mechanisms of PZT nanorod and nanohexagon formation are proposed. In Chapter 6, a conclusion for this project as well as suggestions for future work is presented. Overall, this thesis embodies the research work performed at the BINARY laboratory at the University of Alberta since the Fall of 2010. It entails the complete process of a promising technique to produce single-crystalline PZT nanostructures from initial study of different synthesis techniques to the final testing of the produced nanocrystals.

Chapter 2 Approaches for the synthesis of PZT nanocrystals

There are three approaches to get PZT nanocrystals (powder) – conventional method, hydrothermal method and sol-gel method, in which, the last two methods are also regarded as wet-chemical approaches. This Chapter discusses the methods and procedures used to synthesize the PZT nanocrystals in this research project, a comparison among the three approaches is provided at the end of this Chapter.

2.1 Conventional methods

PZT powders were conventionally synthesized by the solid-state reaction process by using oxides as raw materials [6]. However, this process requires a fairly high temperature that can cause significant loss of lead oxide, and results in the poor performance of PZT ceramics [7–9]. The conventional process also has some other disadvantages, for instance, compositional inhomogeneity, impurity introduced during the milling and large particle size. All these drawbacks lead to the degradation of the performances of the final PZT ceramics [10]. Therefore, some specific wet-chemical routes have been developed to prepare high-quality PZT powders, such as hydrothermal, sol–gel and other chemical processes.

2.2 The Sol-gel method

2.2.1 Introduction of sol-gel synthesis

Sol-gel process, a wet-chemical technique, has been widely used in the fields of ceramic engineering and materials science. This is a method mainly used for the synthesis of materials (typically metal oxides) starting from a "sol" (colloidal solution) that acts as the precursor for a "gel" (integrated network of particles or polymers). Metal alkoxides and metal salts are typical precursors , for example: chlorides and nitrates andacetates, which have various forms of hydrolysis and polycondensation reactions. If sol-gel process can be properly carried out, it offers us with excellent control and reproducibility of process chemistry. Since the 1990s, sol-gel method is becoming an important research area, in which more than 35,000 papers have been published worldwide on this process [11, 12, 13]. The interest in sol-gel processing can be further traced back in the mid-1980s, the observation of the TEOS, which is short for hydrolysis of tetraethyl orthosilicate, under acidic conditions led to the formation of SiO_2 in the form of monoliths and fibers. In ceramics processing and manufacturing, it can be used as an investment casting material, or as way of producing very thin films of metaloxides.

The sol-gel approach, which is a cheap and low-temperature technique, allows for the fine control of the chemical composition of products. Even some small quantities of dopants like organic dyes and rare earth elements can be introduced in the sol and dispersed uniformly in the final product. In this particular chemical procedure, the solution (sol) gradually evolves towards the formation of a gel-like

system containing a liquid phase and solid phase whose morphologies ranging from discrete particles to continuous polymer networks. In the case of the colloid, since the volume fraction of particles (or particle density) may be quite low, a significant amount of fluid needs to be removed initially for the gel-like properties to be recognized. This can be accomplished in different ways, and the simplest method is to allow time for sedimentation to occur, followed by pouring off the remaining liquid.

A drying process is required to remove the remaining liquid (solvent) phase requires, which is typically accompanied with a significant amount of shrinkage and densification. Clearly, the ultimate microstructure of the final component will be strongly influenced by the changes imposed on the structural template during this phase of processing. The rate at which the solvent can be removed is finally determined by the distribution of porosity in the gel. Afterwards, a thermal treatment (firing process) is often needed in order to favoring further polycondensation and enhancing mechanical properties and structural stability via final sintering, densification and grain growth. Compared to the traditional processing techniques, one of the most distinct advantages of using this methodology is that densification is often achieved at a much lower temperature.

The precursor sol can be either used to synthesize powders (microspheres and nanospheres) or deposited on a substrate to form a film (e.g., by dip coating or spin coating). The sol-gel methods, has derived lots of materials which have diverse

applications in electronics, space, energy, space, biosensors, optics, reactive material and controlled drug release.

2.2.2 Nanoscale materials

Microstructural inhomogeneities [14, 15] can be given rise by uncontrolled flocculation of powders due to attractive van der Waals forces. The irregular particle shapes and sizes in a typical powder usually result in non-uniform packing morphologies in the processing of fine ceramics, leading to packing density variations in the powder compact.

Any fluctuations in packing density in the compact as it is prepared for the kiln are often increased in the sintering process, which yields inhomogeneous densification. Some pores and other structural defects with density variations have been proved to play an important role in the sintering process by growing and then limiting end-point densities. The development of differential stresses which as a result of non-uniform drying shrinkage are directly related to the rate at which the solvent can be removed, thus highly depend on the distribution of porosity. Such stresses have been associated with a plastic-to-brittle transition in consolidated bodies [16]. If not relieved, it can yield to crack propagation in the unfired body. Differential stresses coming from inhomogeneous densification have also been proved to result in the propagation of internal cracks, where the strength-controlling flaws take place [17-21].

The total control over particle-particle interactions is required by the containment of a uniformly dispersed assembly of strongly interacting particles in suspension. Monodisperse colloids have this potential [22, 23, 24]. For example, monodisperse powders of colloidal silica may be sufficiently stabilized to ensure a high degree of order in the aggregation resulting colloidal crystalor polycrystalline colloidal solid. The time and space allowed for longer-range correlations to be established appears to limit the degree of order. Such defective polycrystalline structures would be the basic elements of nanoscale materials science, and thus providing the first step in the development of a more rigorous understanding of the mechanisms, which involved in microstructural evolution in inorganic systems such as sintered ceramic nanomaterials [25, 26].

2.2.3 Liquid phase and solid phase

In sol-gel process, the sol evolves gradually form a gel-like network, which contains a liquid phase and a solid phase. For the solid phase, its basic structure or morphology range anywhere from discrete colloidal particles to continuous chain-like polymer networks [27, 28]. Normally, precursors are metal alkoxides and metal chlorides, which undergo hydrolysis and polycondensation reactions to the formation of a colloid. They contain distinct solid (or liquid) particles which disperse to various degrees in a liquid medium. Colloid is a term that generally used to describe a wide range of solid-liquid (or liquid-liquid) mixtures. It is specific to the individual particles, which are small enough to exhibit Brownian motion but larger than atomic dimensions. The diameter of this critical size particle usually

ranges from tens of angstroms (10^{-10} m) to a few micrometres (10^{-6} m) [29]. The dynamic behavior of these particles in any period of time in suspension would be governed by gravity forces and sedimentation if the particles are large enough. Ceramic powders of a wide range of chemical composition can be formed uniformly due to precipitation. However, as described originally by Albert Einstein in his dissertation, their irregular motion in suspension can be attributed to the collective bombardment of a myriad of thermally agitated molecules in the liquid suspending medium if they are small enough to be colloids. This erratic behavior could easily be described using the theory of Brownian motion, with sedimentation being a possible long term result, concluded by Einstein.

The particles may grow to enough size to become colloids, which are affected by gravity and sedimentation under certain chemical conditions, normally in base-catalyzed sols. Stabilized suspensions of such sub-micrometre spherical particles may result in self-assembly—yielding highly ordered microstructures reminiscent of the prototype colloidal crystal, which is called precious opal [22, 23]. The inter-particle forces have sufficient strength to cause considerable aggregation or flocculation prior to their growth under certain chemical conditions, typically in acid-catalyzed sols. The formation of an open continuous network of low density polymers shows certain advantages with regard to physical properties in the formation of high performance ceramic or glass components in 2 and 3 dimensions [30].

In the cases of both discrete particles and continuous polymer network, the drying

process serves to remove the liquid phase from the gel, yielding a micro-porous amorphous glass or micro-crystalline ceramic. In order to favor further polycondensation and enhance mechanical properties, subsequent thermal treatment, like sintering, may be performed. On the other hand, in the case of either discrete particles or continuous polymer network, the sol evolves gradually towards the formation of an inorganic network, which contains a liquid phase (gel). Formation of a metal oxide includes connecting the metal centers with oxo (M-O-M) or hydroxo (M-OH-M) bridges, which generates metal-hydroxo or metal-oxo polymers in solution. Both of the optical quality glass fiber and refractory ceramic fiber can be drawn within the viscosity of a sol adjusted into a proper range, which are used for thermal insulation and fiber optic sensors.

2.2.4 Gelation

It can be shown that even most simple liquids will display some elastic response at shear rates or frequencies exceeding 5 x 10^6 cycles per second. The response of a gel to an oscillation or vibration will depend on the period or frequency of vibration in a dynamic sense. The fundamental motions of the primary particles (or particle clusters) have been probed by experiments on such short time scales which constitute the aggregate or lattice structure. One of the manifestations of this phenomenon is the increasing resistance of certain liquids to flow at high stirring speeds. Therefore, the ability of a condensed body to respond to a mechanical force by viscous flow is strongly dependent upon the time period over which the load is applied, and also the amplitude and frequency of the stress wave in oscillatory

experiments [31, 32].

Polymeric gels are able to propagate shear waves with relatively low damping has been shown theoretically in a certain range of low-frequency. The difference between a sol and a gel thus appears to be understood in a manner similar to the practical difference between the elastic and plastic deformation ranges of a metal. The difference lies in the ability to respond to applied shear force via macroscopic viscous flow [33, 34]. The prime difference between a liquid and a solid, in a static sense, is that the solid has elastic resistance against a shearing stress while a liquid does not have. Normally, a simple liquid will not support a transverse acoustic phonon or shear wave.

Phase transition

The discrete and reversible volume transitions which occur in partially hydolyzed acrylimide gels are able to be interpreted in terms of a phase transition of the system, which consists of the charged polymer network, hydrogen (counter)ions and liquid matrix. The volume change at the transition point is either discrete or continuous, which meanly depend on the degree of ionization of the gel and on the solvent composition [35-38].

The sum osmotic pressure of the gel is same as the total osmotic pressure acting on the system. There are three forces which contribute to the osmotic pressure in the gelation, which are:

1) The negative pressure due to polymer-polymer affinity;

2) The positive osmotic pressure of (+) hydrogen ions;

3) The rubber-like elasticity from the network of polymers.

The phase transition is a manifestation of competition among these three forces. The balance among these forces varies with the temperature changing or solvent properties. It is further conformed that the phase transition can be induced by applying an electrical field across the gel.

Structural relaxation

The structural relaxation of a viscoelastic gel has been described as primary mechanism responsible for densification and associated pore evolution in both of the colloidal and polymeric silica gels [11]. In order to handle the polymer solutions, liquids and gels and the determination of their viscoelastic properties, high frequencies with ultrasonic waves have been used extensively. A force varying with a frequency (or period) appropriate to the relaxation time of the phenomenon investigated, and inversely proportional to the distance over such relaxation occurs is required by the experiments in the viscoelastic properties of such skeletal networks on various time scales. In order to monitoring the dynamics of density fluctuations through the behavior of the autocorrelation function near the point of gelation, Dynamic Light Scattering (DLS) techniques have been used. The static measurements of the shear modulus have then been made [39-44], it is a measurement that yields the dynamic modulus of rigidity.

Ultimate microstructure

The difference in average size between the smaller pores (in regions of higher average density) and the larger pores (in regions of lower average density) will depend on the degree of phase separation, which is allowed to occur before such fluctuations become thermally arrested around or at the critical point of the

transition. If the restoring force, which depends on the network elasticity, is large or if the friction between the network and the interstitial fluid is small, the rate of relaxation of density will fluctuate rapidly. The rate is proportional to the elasticity and inversely proportional to the frictional force, which is illustrated by the theory. Thus the friction depends on both of the fluid's viscosity and the pores' average sizes contained within the polymer network.

Elastic continuum

The gel is acted as an elastic continuum deforming when subjected to externally applied shear forces, however, is incompressible upon application of hydrostatic pressure. Direct experimental access to measurement of the wavelength and lifetimes of critical fluctuations are offered by quasi-elastic light scattering, which are dominated by the viscoelastic properties of the gel. An expectation of the relationship between the amplitude of such fluctuations and the elasticity of the network will be reasonable. The elasticity approaches zero, or the compressibility becomes infinite is implied by the divergence of the scattered light intensity at a finite critical temperature, which is a typically observation of the behavior of a system at the point of instability. The fluctuations should grow larger as the elasticity declines, because the elasticity measures the resistance of the network to elastic (reversible) or plastic (irreversible) deformation. Therefore, the polymer network offers no resistance at all to any form of deformation at the critical point. Infinite expansion or contraction within the network may be produced by the thermal fluctuations, and the molecular morphology and the degree of hydration of the body will be ultimately determined by the evolution of such fluctuations. The

combination of fluidity and rigidity can be described as the gel structure: that of a liquid included in a fibrous matrix or polymer network by the extremely large friction between the liquid and the fiber or polymer network.

2.2.5 Applications of sol-gel method

The applications for the products derived by sol-gel are numerous [45-50]. For instance, the world's lightest materials and some of its toughest ceramics have been produce by using it. Some concrete applications of sol-gel method have been reported as follows:

Nanoscale powders

Lots of composite powders have been patented for the applications of agrochemicals and herbicides. Powder abrasives, for example, have used in a wide range of finishing operations. Carrying out zeolite synthesis is another important application of sol-gel processing. Precipitation is able to form ultra-fine and uniform ceramic powders, these powders of single and multiple component compositions can be fabricated on a nanoscale particle size for biomedical applications. Other elements, like metals and metal oxides, can be easily incorporated into the final product and it can form very stable silicate sol.

An extremely porous and highly low density material called aerogel will be obtained if the liquid in a wet gel is removed under a supercritical condition. The gel is dried by means of low temperature treatments (25-100 °C), it is possible to obtain xerogels that has porous solid matrices. Other products produced by this process include various ceramic membranes for microfiltration, nanofiltration and

ultrafiltration. A sol-gel process for the production of radioactive powders of UO_2 and ThO_2 was developed in the 1950s, for nuclear fuels without generation of large quantities of dust.

There are also some other applications in research, one is to entrap biomolecules for biosensors or catalytic purposes by physically or chemically preventing them from leaching out and, by shielding them from the external environment which monitoring small molecules, in the case of chemical-linking small molecules or protein. However, there are some drawbacks of this application. For instance, the change in local environment may change the functionality of the protein and the synthesis step may damage the protein as well. Various strategies have been explored to circumvent this disadvantage, for example: monomers with protein friendly leaving groups (like glycerol) and the inclusion of polymers which stabilize protein (like PEG) [51].

Opto-mechanical

The researchers at the Fraunhofer Institute for Ceramic Technologies and Sintered Materials have developed one example of an opto-mechanical material. Even though the sintered alumina nanomaterial is very hard and virtually transparent over a range of wavelengths, it can be synthesized at temperatures from 1000 to 1200 °C, which is much lower than its melting point (2070 °C) like other sintered materials which using larger particles of larger diameter and less sophisticated processing methodologies. It is the microscopic pores in sintered ceramic nanomaterials, mainly trapped at the junctions of microcrystalline grains that who cause light to scatter and prevented true transparency. The total volume fraction of

these nanoscale pores (intergranular and intragranular porosity) has been observed to be less than 1% for high-quality optical transmission [52, 53].

Sol-gel route is a quick and cheap way to make macroscopic optical elements, active optical components as well as large area of hot mirrors, cold mirrors, lenses and beam splitters. A translucent or even transparent materiala can be made due to the reduction of the original particle size below the wavelength of visible light (~ 500 nm) eliminates much of the light scattering. In the processing of high performance ceramic nanomaterials which has superior opto-mechanical properties under adverse conditions, the size of the crystalline grains is meanly determined by the size of the crystalline particles present in the raw material during period of forming the object.

Thin films and fibers

Many ceramic materials, glassy and crystalline for example, have been found applications in various forms from bulk solid-state components to high surface area forms such as coating, fiber and thin film [30, 54]. Both of the optical and refractor ceramic fibers can be drawn with the viscosity of a sol adjusted into a proper range, which can be used for fiber optic sensors and thermal insulation.

Protective coatings

Thin film is one of the largest application areas that it can be produced on a piece of substrate by dip coating or spin coating. Casting into a mold followed by drying and heating treatment, dense ceramic or glass articles with novel properties can be formed, which can not be produced by any other method. Decorative coatings, protective coatings and electro-optic components can be applied to glass, metal and

other kinds of substrates with these methods. There are some other coating methods like spraying, electrophoresis, inkjet printing and roll coating.

2.3 Hydrothermal method

2.3.1 Introduction of Hydrothermal

The use of the hydrothermal technique to produce thin films of PZT on substrates has some advantages over sol-gel and sputtering in that curved surfaces can be coated [55, 56, 57] and a variety of substrate materials can be used [58]. Hydrothermal synthesis is a method of synthesis of single crystals which depends on the solubility of minerals in hot water under high pressure. An apparatus consisting of a steel pressure vessel called autoclave is used to perform the crystal growth, in which a nutrient is also supplied along with water. In order to take additional growth when the hotter end dissolves the nutrient and the cooler end causes seeds, a gradient of temperature is maintained at the opposite end of the growth chamber. During the development of the hydrothermal technique, there are lots of techniques to synthesize PZT with initial studies producing a mixture of lead titanate and lead zirconate. The basic hydrothermal procedure was first proposed by Deng et al. [59] for the synthesis of PZT. It is a relatively simple technique that utilizes the following precursors in powders [60]: Lead nitrate—$Pb(NO_3)_2$, Zirconyl oxychloride—$ZrOCl_2 \cdot 8H_2O$ and Titanium dioxide —TiO_2.

Even though a metal substrate is much better way to the ease of fabrication than a single crystal substrate high-quality epitaxial PZT or $PbTiO_3$ thin films are able to

be deposited on a single crystal substrate such as $SrTiO_3$ [61, 62], which has superior lattice matching to PZT or $PbTiO_3$ and high resistance against strongly alkali conditions. High-quality piezoelectric film can be deposited by the hydrothermal method. The ferroelectric and the piezoelectric properties were successfully measured by improving the reaction conditions and adapting the $SrRuO_3$ bottom electrode on $SrTiO_3$ [63]. Polycrystalline PZT can be obtained on a titanium metal substrate [64].

Hydrothermal method has several possible advantages over other types of crystal growth, including the ability to grow materials which have a high vapour pressure near their melting points. The growth of large good-quality crystals while maintaining good control over their composition is also particular suitable for this method. Hydrothermal method is also able to create crystalline phases which are not stable at the melting point. Even though it has lots of merits, we should not turn a blind eye on the disadvantages, which including the need of expensive autoclaves, and the impossibility of observing the growth of the crystal.

2.3.2 History of hydrothermal synthesis

Hydrothermal synthesis includes various techniques, which crystallize substances from high-temperature aqueous solutions at high vapor pressures; also called "hydrothermal method". In 1839, the chemist Robert Bunsen, who came from Germany, contained aqueous solutions in thick-walled glass tubes at the temperatures above 200 °C and pressures above 100 bars [65]. It is the first use of hydrothermal aqueous solvents as media that the crystals of barium

carbonate and strontium carbonate which he grew under these conditions. Geologic is the origin of the term "hydrothermal". Schafhäult in 1845 and de Sénarmont in 1851, who produced microscopic crystals [66], were some other early reports of the hydrothermal growth of crystals. Hydrothermal phase equilibria have been studied by geochemists and mineralogists from the beginning of the twentieth century. Literatures on the growth of macroscopic crystals [67] were later reported by G. Spezzia (1905). Solutions of sodium silicate, natural crystals as seeds and supply, and a silver-lined vessel have been used by him. The hotter part of the vessel was at the top, which is quite different from the modern practice. He successfully produced about 15 mm of new growth over a 200 day period by heating the supply end of his vessel to 320-350 °C, and the other end to 165-180 °C. George W. Morey at the Carnegie Institution and Percy W. Bridgman at Harvard University did much of the work , which laid a good foundation of the containment of reactive media in the temperature and pressure range where a majority of the hydrothermal work is conducted. There are some other notable contributions, which have been made by Nacken (1946), Hale (1948), Brown (1951), Walker (1950) and Kohman (1955) [68]. Deng et al. [59] produced 52:48 PZT by adding stoichiometric quantities of the precursors to a home-built autoclave with 100 ml capacity in their paper. The best piezoelectric and ferroelectric properties of PZT can be achieved near the morphotropic phase boundary (MPB), where the Zr/Ti ratio is approximately 52/48 at room temperature [69].

2.3.3 Hydrothermal techniques

Metastable-phase technique

This is a technique which is based on the difference in solubility between the phase to be grown and serving as the starting material. In general, metastable phase's solubility exceeds the solubility of the stable phase, and the latter one crystallizes due to the dissolution of the metastable phase. Metastable-phase technique is usually combined with one of the other two techniques which have been mentioned above. The compounds which are thermodynamically unstable under the growth conditions are consisted in the nutrient.

Temperature-reduction technique

Crystallization takes place without a temperature gradient between the growth and dissolution zones in this method. The following is the reason why this method is not commonly used. Even though a gradual reduction in temperature of the solution in the autoclave successfully achieves the super saturation, it is hard to in control the growth process and introducing seed crystals.

Temperature-difference technique

Temperature-difference method is the most widely used method in the processes of hydrothermal synthesis and crystal growing. The nutrient is placed in the lower part of the autoclave where filled with a certain amount of solvent, and the autoclave is sintered in order to create two different temperature zones. Reducing the temperature in the crystal growth zone can successfully achieve the super saturation. Because of the reduction in temperature and crystallization sets in, the solution

becomes supersaturated in the upper part. The nutrient will be dissolved in the hotter zone and the saturated aqueous solution which stand in the lower part will be transported to the upper space by convective motion of the solution. The counter flow of solution inclines while the cooler and denser solution in the upper part of the autoclave declines.

2.3.4 Equipments

Autoclaves are used as the vessels of crystallization, they are thick-walled steel cylinders with a hermetic seal, which normally have to be able to withstand high temperatures and pressures for prolonged periods of time. Mostly, steel-corroding solutions are used in the process of hydrothermal experiments. Generally, the material of autoclaves must be inert with respect to the solvent, the most important element of the autoclave is the closure. Various designs have been produced for seals, the Bridgman seal is the most famous one. Protective inserts are generally used, in order to prevent corrosion of the internal cavity of the autoclave. Depending on the temperature and solution used, different inserts may be made of silver, gold, carbon-free iron, copper, titanium, quartz or Teflon. They may have the same shape of the autoclave and may fit well in the internal cavity (contact-type insert) or be a "floating" type insert, the type which occupies only part of the autoclave interior.

2.3.5 Applications

Hydrothermal synthesis is always used to grow synthetic quartz, gems and other

single crystals with high commercial value. Figure 2.1 shows a synthetic quartz crystal grown by the hydrothermal method**.** Some of the crystals, which have been efficiently grown, are emeralds, rubies, quartz, alexandrite etc. A large number of compounds belonging to almost all classes have been fabricated under hydrothermal conditions, like: tungstates, molybdates, carbonates, silicates and germanates. Hydrothermal synthesis has proved to be extremely effective both in the systematic physicochemical investigation of intricate multicomponent systems at elevated temperatures and pressures and also in the search for new compounds with specific physical properties.

Figure 2.1 A synthetic quartz crystal grown by the hydrothermal method

2.4 Comparison

In table 2.1, a briefly comparison has been made among different methods.

Table 2.1 Advantages and disadvantages of different synthesis approaches

Comments/ Methods	Conventional Method	Hydrothermal method	Sol-gel Method
Advantages	Traditional method Simple	1.Low cost 2.Lowest temperature	1. Lower sintering temperatures. 2.Shoter reaction time 3.Recyclable solution
Disadvantages	1. Loss of lead oxide 2.Compositional inhomogeneity 3.large particle size	1.Difficult to avoid intermediate phases 2.Poor dielectric and piezoelectric properties 3.Long reaction time 4.Need waste water treatment	Toxic organic solvent

After comparing the merits and drawbacks among different methods and considering the experimental conditions in our lab, the sol-gel method is selected in my research project. Sol-gel processing of making inorganic nanostructural crystals has been proved to be quite successful due to its higher degree of homogeneity comparing to the other methods [70]. The sol–gel process requires lower reaction

temperatures than the traditional soft chemistry methods. The method allows the production of solid material from liquid by using a sol or a gel as an intermediate product. In sol-gel process, thin films or fibers could be directly made from solution by powderless processing of glasses or ceramics. Sol–gel chemistry which is based on the transformation of molecular precursors into an oxide network by condensation reactions is often involved in the synthesis of solid materials via ‘soft chemistry’ process [71, 72]. Moreover, sol-gel routes have made it possible to obtain very thin ferroelectric films with splendid operational and structural characteristics for several applications [70].

Chapter 3 Synthesis of PZT nanocrystals

Discussions of solution preparation and solvent selection are made in chapter 3. With the aid of the prepared solution and the selected solvent, PZT nanocrystals have been made by sol-gel method. The composition of the fabricated PZT nanocrystals is investigated by X-ray diffraction (XRD) and Raman spectra, and the morphology of the prepared PZT nanocrystals is investigated by atomic force microscope (AFM) and transmission electron microscopy (TEM).

3.1 Preparation of solution

The way to prepare solution is very important for the synthesis of PZT nanocrystals. Solution chemistry variations, like differences in precursor structure or solvent, are able to play a significant role in the processing of the as-deposited film. Besides the characteristics of precursor, film processing behavior (substrate wetting) can also have important impact on the determination of the developed solution chemistry. In order to synthesize perovskite thin films, the most commonly used chemical solution deposition (CSD) methods may be classified into three categories:

(1) Chelate processes, with modified ligands like acetic acid [73, 74, 75];

(2) Sol-gel processes, with 2-methoxyethanol as a reactant and solvent [76, 77, 78], the reactivity of the reagents is relatively high in some practical sol-gel processes;

(3) Metalloorganic decomposition (MOD) routes, with metal carboxylate compounds which are insensitive to water [79, 80, 81]. The structure of the species

in solution will not be the same as the starting compounds if alcohol exchange happens or some modified ligands are used.

The nature of the solution precursors and gels may be controlled by manipulating the reflux, catalysis, and hydrolysis conditions, which allow us to control the properties of material. Some reports show that the precursors formed in the lead zirconate titanate and lead titanate deposition solutions small and mixed metal oligomers [78, 82] while other reports demonstrate that the A-site precursor may not be tightly linked with the formation of the gel network [83, 84]. In particular, the results shown in [83] for Extended X-ray Absorption Fine Structure (EXAFS) tests of PZT gels illustrate that Ti- O-Ti, Zr-O-Ti, and Pb-O-Pb exist separately within the gel structure, which means that "intimate" mixing of the starting reagents has not occured. Metalloorganic compounds, which dissolved in a common solvent, are usually used in solution preparation of perovskite materials. The starting reagents are described as follows:

$M(OR)_x$, metal alkoxide compounds;

$M(OOCR)_x$, metal carboxylates;

$MO_x(CH_3\text{- }COCHCOCH_3)_x$, metal β-diketonates.

In which, "M" represents a metal and "R" represents an alkyl group,

Preparing a "homogeneous" solution that may be applied to a substrate is the general principle of the solution deposition of perovskite films. The synthesis of thin films by this approach has four steps:

1. Fabrication of the precursor solution;

2. Deposition by spin-casting, in which drying process typically start depending on the solvent;

3. Higher temperature heating condition for densification, crystallizing the coating into the desired oxide phase by applying 600-1100 °C.

4. Low-temperature heating condition for drying, pyrolysing organic species around 300-400 °C, and forming of an amorphous film;

5. Generally, the final three steps are similar in spite of differences in the characteristics of the precursor solution for most of the solution deposition methods.

3.2 Solvent

2-methoxyethanol [76, 77] is the most appropriate solvent for sol-gel processes, in which the key reactions of the precursors are hydrolysis and condensation as follows:

Hydrolysis: $M(OR)_x + H_2O$——$M(OR)_{x-1}(OH) + ROH$

Condensation (water elimination): $2M(OR)_{x-1}(OH)$ ——$M_2O(OR)_{2x-2} + H_2O$

Condensation (alcohol elimination): $2M(OR)_{x-1}(OH)$——$M_2O(OR)_{2x-3}(OH) + ROH$

Even though other alcohols have also been utilized, 2-methoxyethanol (CH_3-OCH_2CH_2OH) is the most extensively used solvent in the chemical synthesis of perovskite materials. It is belonging to a class of solvents called glycol

ethers which are famous for their capability to dissolve different types of chemical compounds. 2-Methoxyethanol or methyl cellosolve is an organic compound, which is clear, colorless liquid with an ether-like odor. Although 2-Methoxyethanol is toxic to the bone marrow and testicles, it has been used as a solvent for many different purposes such as varnishes, dyes or resins. It can be produced by the methanol's nucleophilic attack on protonated oxirane followed by proton transfer. 2-Methoexethanol is usually used as a solvent, which can be mixed with water and other solvents.

3.3 Experiments

PZT crystals with a composition of $Pb(Zr_{0.52}Ti_{0.48})O_3$, which are near the morphotropic phase boundary and show superior dielectric and piezoelectric properties[85], were synthesized by a modified sol-gel method[86]. The starting materials were zirconium nitrate $ZrO(NO_3).6H_2O$, lead acetate hydrate $Pb(CH_3COO)_2.3H_2O$ and titanium isopropoxide $Ti(OC_4H_9)_4$. In this process, the ratio of Pb:Zr:Ti was 1:0.52:0.48, all of the chemical reagents used were purchased from Sigma- Aldrich USA of analytical grade and were used without further purification. The system which is designed for the fabrication of PZT powders is shown in Figure 3.1.

Figure 3.1 System for fabricating PZT powders

First of all, $Pb(NO_3)_2$ and $ZrO(NO_3).6H_2O$ were initially dissolved in 2-methoxyethanol and stirred at 100°C for 30 minutes to get a transparent solution. Secondly, $Ti(OC_4H_9)_4$ was added into the precursor, and the mixture was stirred at 150°C for 2 hours to form PZT-sol. The PZT-sol was then stirred and distilled at 125°C under slight vacuum for solvent removal and homogeneity purpose. During this process, a light yellow gel was obtained after 3 hours. The viscous PZT-gel was continued to remove 2-methoxyethanol under vacuum condition for 18 hours to get the totally dried PZT-gel. After cooling down to room temperature, the dried gel was crushed into fine PZT powders.

Figure 3.2 The kiln used for sintering

The PZT nanocrystals were achieved by sintering the PZT powders at 700°C for 24 hours in a kiln. Figure 3.2 shows the kiln in which the PZT powders are sintered. The detailed information about the fabricating process of PZT nanocrystals was shown in Figure 3.3. Some of the PZT nanocrystals were carefully selected and analyzed by Atomic Force Microscope (AFM), X-Ray Diffraction (XRD) and transmission electron microscopy (TEM).

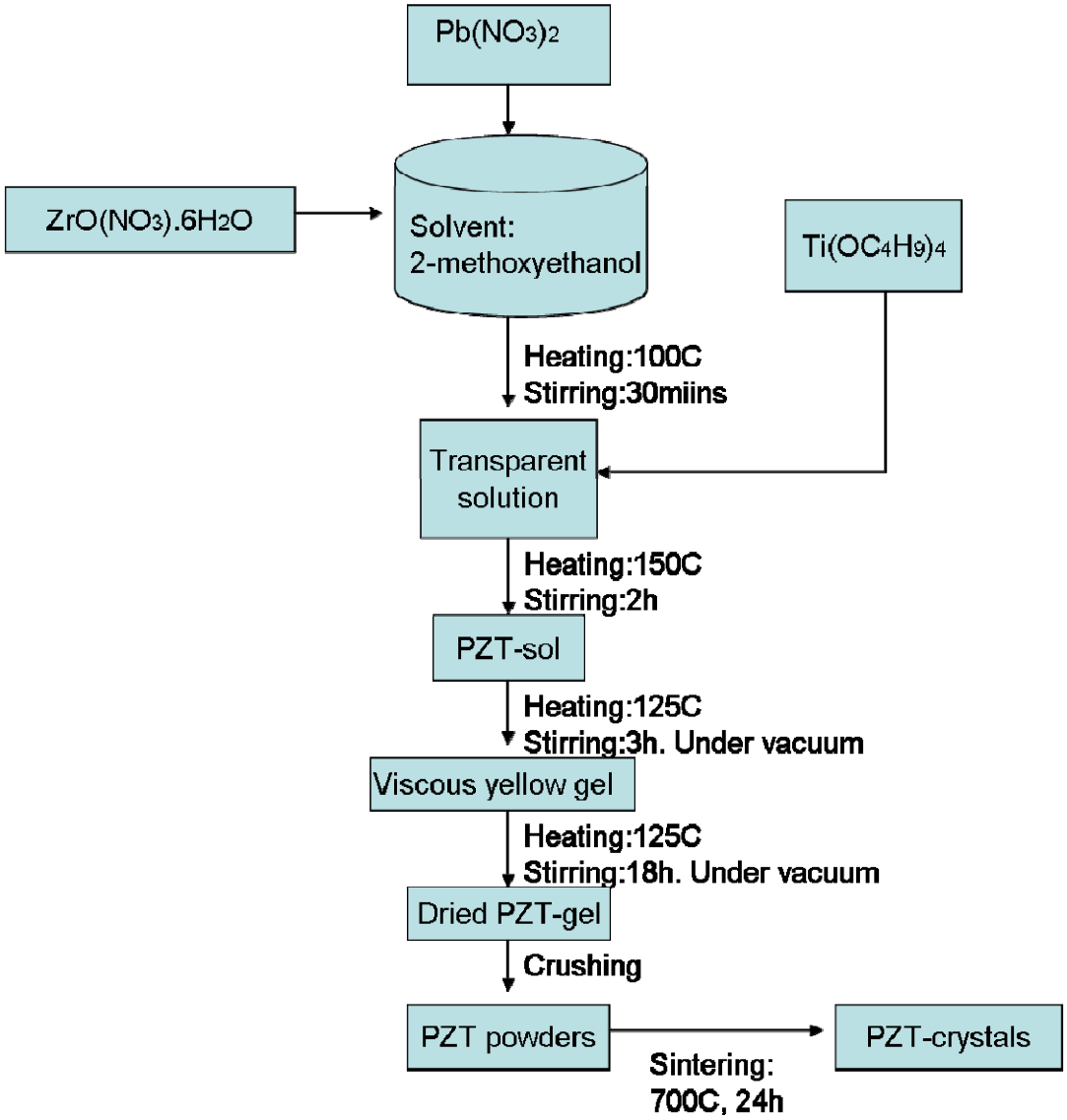

Figure 3.3 Process of synthesizing PZT nanocrystals

3.4 Results

XRD pattern of PZT particles

Here we report the results of nanostructural investigation of the as-prepared PZT nanocrystals. X-ray diffraction (XRD) pattern of the synthesized PZT powders is displayed in Figure 3.4. The result from XRD shows that the PZT powders are in

the composition of $Pb(Zr_{0.52}Ti_{0.48})O_3$, which stand at morphotropic phase boundary (MPB), just exactly the same as our expectation. The sharp and strong reflection peaks in Figure 3.4 illustrate the prepared PZT particles have been highly crystallized during the sintering process. It can be clearly seen that all the diffraction lines are perfectly assigned to monoclinic phase with no other peaks have been observed, which is in a good agreement with the literature value (PDF No.97-009-7062). It can be concluded that the fabricated PZT nanocrystals are of monoclinic perovskite structure, which illustrate that the PZT nanocrystals are of highly compositional homogeneity.

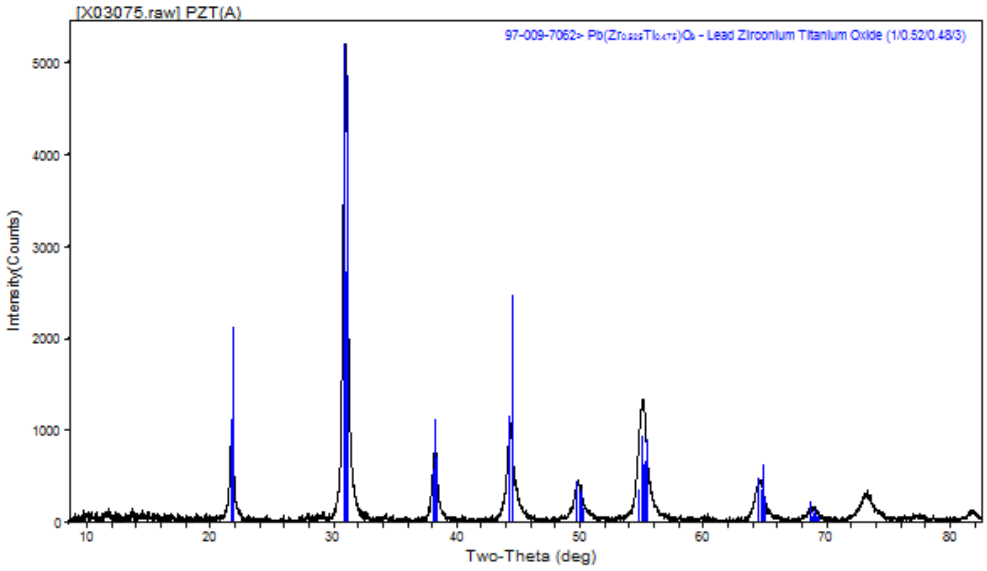

Figure 3.4 XRD pattern of PZT nanocrystals

Raman spectra of PZT crystals

Figure 3.5 shows the Raman spectra of PZT crystals. Following parameters were used for the tests: 1) Excitation laser wavelength: 780 nm; 2) exposure time: 10sec; 3) Charge Coupled Device (CCD) detector; 4) backscattering geometry. The

Raman shift peaks of PZT crystal located at around 206, 281, 332, 556 and 740cm^{-1}, which correspond to E(2TO), ET+B_1, A_1(2TO), A_1(3TO) and A_1(3LO) respectively and match the typical Raman peaks of perovskite PZT [87, 88]. The result from Raman spectra gave us evidence that PZT crystals had been successfully fabricated.

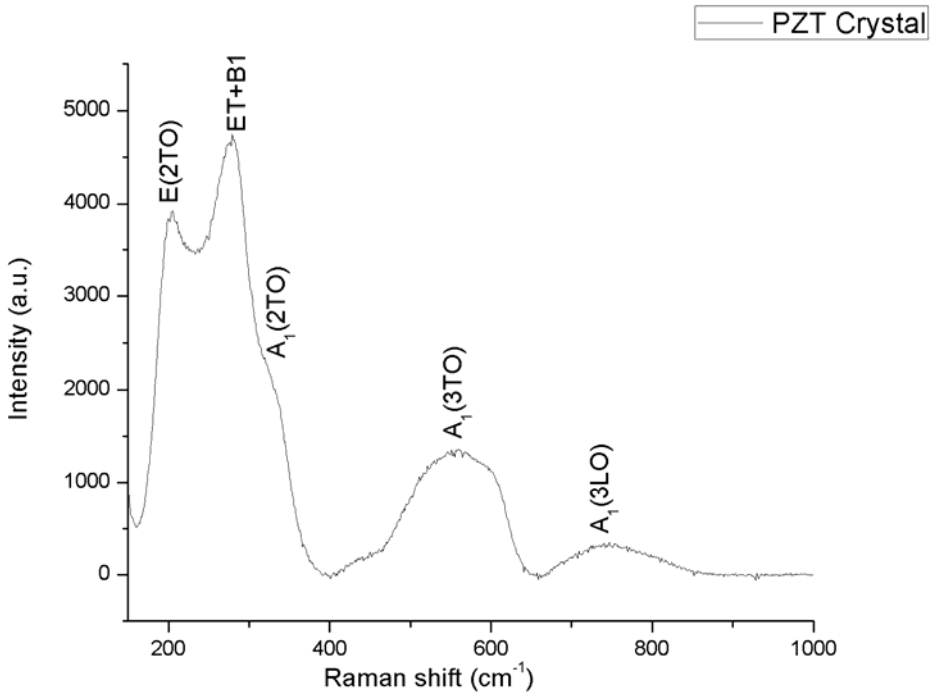

Figure 3.5 Raman spectra of PZT crystal.

AFM investigation of PZT nanocrystals

Then, the PZT powders were investigated by an Atomic Force Microscope (AFM) and the result is shown in Figure 3.6. The procedures of making a sample of PZT crystals for AFM testing are described in the following lines. The main idea was to prepare PZT sample without chemical reaction on the sub, thus the PZT crystals were dispersed by DI water. PZT crystals of desired composition had been already fabricated and were deposited on the silicon chip from an appropriate suspension.

The as-prepared sample was then put into incubator for a thermal treatment at 60 ^{o}C for 4 hours to remove the water. AFM was under tapping-model with a scanning rate of 0.7um/s. From the picture took by AFM, it is easy to see many very small individual particles dispersed uniformly on the silicon chip. The particles are of submicon size, most likely in nanoscale. The mean crystallite size of the PZT powders was then calculated by high resolution transmission electron microscopy (HR-TEM).

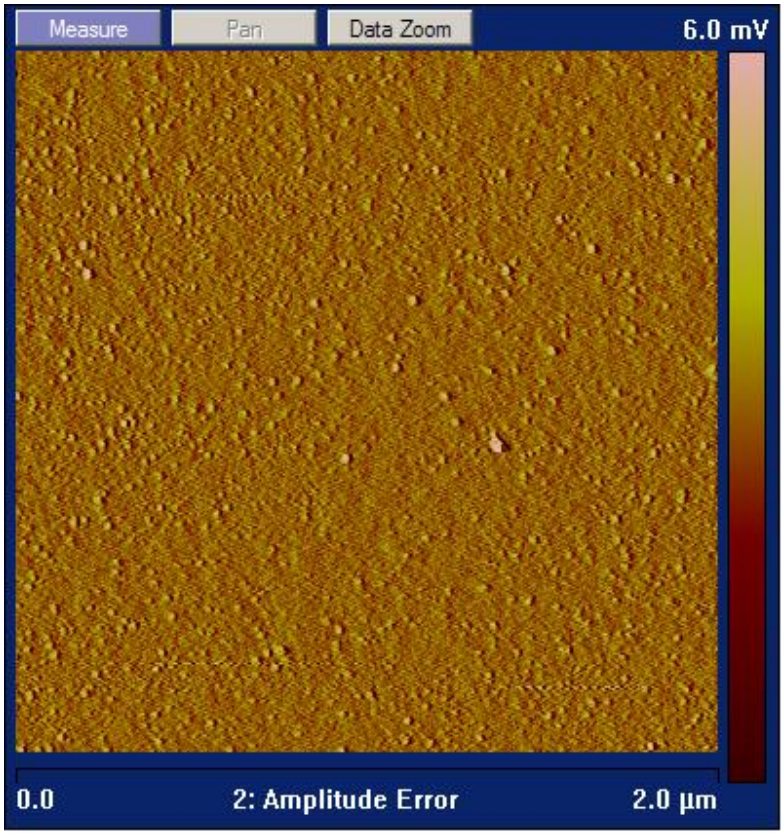

Figure 3.6 AFM image of PZT nanocrystals

TEM images of PZT nanocrystals

Transmission Electron Microscopy (TEM) image and its corresponding Selected Area Electron Diffraction (SAED) pattern of the as-prepared PZT nanocrystals are

shown in Figure 3.7. By taking an overview of this picture, it can be clearly seen that the sample entirely consists of nanosized PZT particles, which are situated individually and no large particles have been observed. Clearly, the nanoparticles are relatively uniform in size and mostly spherical in shape, with an average grain size of 6.8 nm. The diffraction rings in the SAED pattern, which inset in the lower right corner of Fig 3.7, giving us additional evidence that the nanoparticles were highly crystallized.

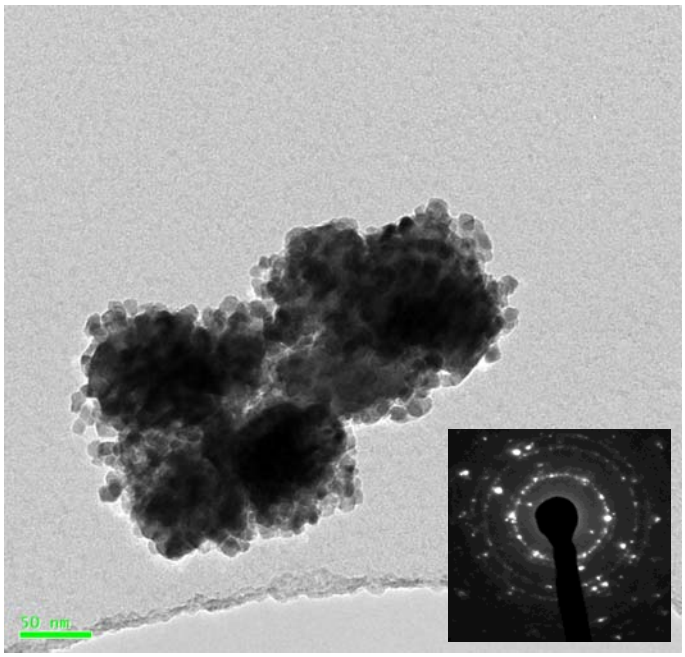

Figure 3.7 TEM image of PZT nanocrystals.

Chapter 4 Synthesis of single-crystalline PZT nanorods and nanohexagons

In Chapter 4, the properties of different types of synthesis tachniques for nanostructures are studied and analyzed to identify a suitable candidate for this project. A salt-surfactant-assisted approach is proposed, and Triton and Tween 20 are selected as the surfactants in this project. With the aid of NaCl and surfactants, single-crystalline PZT nanorods and PZT nanohexagons are successfully fabricated. The properties of crystallization and single crystal are also discussed in this chapter. The characterization of PZT nanorods and PZT nanohexagons are shown at the end of this chapter.

4.1 Introduction

4.1.1 Approaches to fabricating nanostructures

Template-Assisted Synthesis

Generally, template-based synthesis is one of the most common techniques to organize PZT nanocrystals. Using a negative template such as porous alumina or track-etched polymer is the easiest method to produce one dimensional nanostructures of oxides [89, 90]. Their sizes and shapes are controlled by the use

of the porous membrane. The solvent evaporates while the material starts to crystallize on the surfaces of the channels of the template by following a heat treatment. Steven and Seana et al. [91] have grown uniform sized and almost unidirectional aligned PZT nanorods in polycarbonate (PC) membranes with the pore sizes between 100 and 200nm. By using this method, nanotubes are most frequently synthesized, and nanowires have also been reported by increasing the immersion time or employing a particle-directing force such as electrophoresis [92]. PZT nanotubes have been successfully made in nanochannel alumina (NCA) and silicon templates respectively by using pore wetting misted chemical solution deposition[93, 94]. Normally, nanostructure materials are in polycrystalline. Zhang et al. have fabricated $Pb(Zr_{0.53}Ti_{0.47})\ O_3$ nanowires in NCA template via sol-gel process [95]. Electrospinning is another important method which is able to produce a wide range of materials, such as nanofibers or nanowires. Wang et al. made PZT fibers with diameter ranging from 500 nanometers to a few microns by executing metallo-organic decomposition and electrospinning techniques [96]. It can be considered as a template-assisted method, in which the nozzle restricts the polymer solution at the point of fiber formation.

On the other hand, positive templates like nanowires, nanorods, and carbon nanotubes is also capable to produce 1D nanostructures by coating the outside surface of the template with the desired material [89 , 97]. The template itself is able to be converted into the target composition instead of coating the inside or outside surface of a template [97]. However, there are some difficulties in assembling PZT

nanorods, nanotubes, nanofibers or nanowires as functional devices due to the difficulty in producing high-quality ferroelectric nanostructures with controllable size and crystallinity.

Template-Free Synthesis

With the template-free methods it is easier to obtain single-crystalline 1D nanostructures than with the template-assisted methods. A general method for producing well-crystallized nanostructures of perovskite oxides would be of great interest. There are some other approaches to prepare ternary oxides as 1D nanostructures, such as: molten salt synthesis, hydrothermal synthesis and thermolysis. Peng showed that the increasing and removal of metal ions from crystallites were enabled by temperature change due to the rapid absorption and desorption of surfactant molecules from nanocrystal surface [98]. Since one dimensional growth is relatively easy to be obtained for materials with an anisotropic crystal lattice due to the energy difference among different crystal faces, it is quite challenging to identify the exact mechanism for the one dimensional growth without templates. Gang Xu et al. have proposed a polymer-assisted method, which produced 150 to 175 nm wide and 1 to 1.6um long single crystal line tetragonal perovskite PZT nanorods only using poly(vinyl alcohol) (PVA) [99]. They also made 40nm wide and 1.7-3.5um long single crystalline tetragonal perovskite PZT nanowires by combining poly(acrylic acid)(PAA) and poly(vinyl alcohol) (PVA) [99]. Since it can be quite hard to determine the correct set of synthesis parameters that can grow 1D crystal in a system without any inherent driving growth forces, these methods are more like trial-and-error approaches than

the template methods.

Chemical Approaches

The preparation of nanostructures by using chemical methods usually prefers fabrication at lower temperatures than in the fabrication of bulk materials. Generally, the synthesis of nanostructures can generally be divided into two methods: “bottom-up” and “top-down”. More specifically, the bottom-up approach typically uses chemical methods to make nanostructures from individual atoms and molecules get together while the “top-down” approach uses physical methods to downsize big size structures. Physical approach requires great ingenuity to quickly fabricate large quantities of 1D nanostructures from a variety range of materials at fairly low costs, while chemical approach provides us with an different strategy for generating 1D nanostructures due to cost, throughput, and material diversity [100]. Physical top-down methods can be used to fabricate various 1D nanostructures of a wide range of materials, including electron-beam writing, focused-ion-beam writing and nanoimprint lithography.

Diffusion of the reacting species is always a key point for a chemical reaction to occur. Many fabrications of nanoparticle take place at high temperatures and then excessive diffusion is followed by a low and controllable concentration of reactant species. By using pretty small size precursors and a solvent in which the precursors can easily dissolve and diffuse, we can get a sufficient diffusion rate at quite lower temperature. Because of using a solvent instead of solid-state reactions, lots of the chemical methods are called “wet-chemical” methods. The wet-chemical method is

able to mix of the precursors uniformly and reduce the necessary diffusion distance at the same time, which is the main merit of “wet-chemical” method.

4.1.2. One Dimentional Nanostructures

It is necessary to induce anisotropic growth of the material and some selected methods to accomplish such growth for the fabrication of 1D nanostructures by chemical methods. What should be emphasized here is that lots of the literature on 1D nanostructures are pure descriptions of the fabrication, regardless of the growth mechanism. Further applications and nanoscale manufacturing will highly rely on large-scale patterned, designed growth and self-assembly technology. Thus, the control of the number, location and orientation of the one dimentional nanostructures is a primary step in synthesizing nanostructures [101]. It is now possible for many materials in the VLS process of semiconductor nanowires. However, it is still a subject need intensive study for finding other materials and methods. The VLS process happens as follows:

1. A thin (1 to 10 nm) Au film is deposited on a silicon (Si) wafer substrate by thermal evaporation.

2. The wafer is heated at temperatures higher than the Au-Si eutectic point, creating Au-Si alloy droplets on the wafer surface. The melting temperature of the Au:Si alloy reaches a minimum value (around 363 °C) when the ratio is 4:1 Au:Si, which is also known as the Au:Si eutectic point.

3. Lithography techniques may also be used to control the diameter and position of the droplets.

4. 1-D crystalline nanowires can be subsequently grown by a liquid metal-alloy droplet-catalyzed chemical/physical vapor deposition process in a vacuum deposition system.

Since Si has a much higher melting point (approximately 1414 °C) than that of the eutectic alloy, Si atoms precipitate out of the supersaturated liquid-alloy droplet at the interface, and the droplet rises from the liquid-alloy/solid-Si interface.

The vapor–liquid–solid (VLS) or solution–liquid–solid (SLS) method is probably the most popular and controllable method for the preparation of 1D nanostructures, for example: nanowires from chemical vapor deposition. It has especially been widely used to synthesize nanowires of semiconductors such as GaAs, ZnO and Si [100, 101, 102]. The VLS mechanism can be typically described into three stages as follows [103]:

1. Preparation of a liquid alloy droplet on the substrate, where a wire is going to be grown

2. Introduction of the substance to be grown as a vapor, adsorbing onto the liquid surface and diffusing into the droplet

3. Supersaturation and nucleation at the liquid/solid interface, which lead to axial crystal growth.

Since generally the growth of a crystal through direct adsorption of a gas phase on to a solid surface is very slow, the VLS mechanism successfully avoids this by using a catalytic liquid alloy phase which can quickly adsorb a vapor to supersaturation levels, and from which crystal growth can therefore be made

from nucleated seeds at the liquid–solid interface. The physical characteristics of nanowires grown in this manner are controllable, which depend on the size and physical properties of the liquid alloy. Here are some typical features of the VLS process:

1. Highly anisotropic nanowires arrays from a wider range of materials can be produced by this growth mechanism.

2. Much lower reaction energy than normal vapor-solid growth.

3. Nanowires grow in the areas activated by the metal catalysts, and the size and position of the nanowires are determined by that of the metal catalysts.

The requirements for catalysts are illustrated as follows [104]:

1. In order to produce highly directional growth of nanowires, the solid-liquid interface should be crystallographically well-defined.

2. The equilibrium vapor pressure over the liquid alloy should be small, in order to avoid the droplet vaporizing and shrinking in volume.

3. The solid solubility should be low in the solid and liquid phases of the substrate material.

4. Forming a liquid solution with the crystalline material to be grown at the growth temperature of nanowire.

5. Must be examined before choosing a suitable catalyst, because the vapor–solid, vapor–liquid, and liquid–solid interfacial energies have a great influence on the shape of the droplets.

6. Should be inert to the reaction products during the period of nanowire growth.

4.1.3 Oswald Ripening

Ostwald ripening is an observed phenomenon in liquid sols or solid solutions. It demonstrates the phenomenon that small crystals or sol particles dissolve and redeposit onto larger crystals or sol particles over time [105]. In other words, it describes the change of an inhomogeneous structure over a period of time. Wilhelm Ostwald is the first person who reported the dissolution of sol particles or small crystals and the redeposition of the dissolved species onto the surfaces of sol particles or larger particles in 1896 [106]. Ostwald ripening also plays an important role in the area of precipitates digestion, which is an imperative step in gravimetric analysis. In general, the digested precipitate has better purity with easy washing and filtering properties. Figure 4.1 illustrates a basic process of Ostwald.

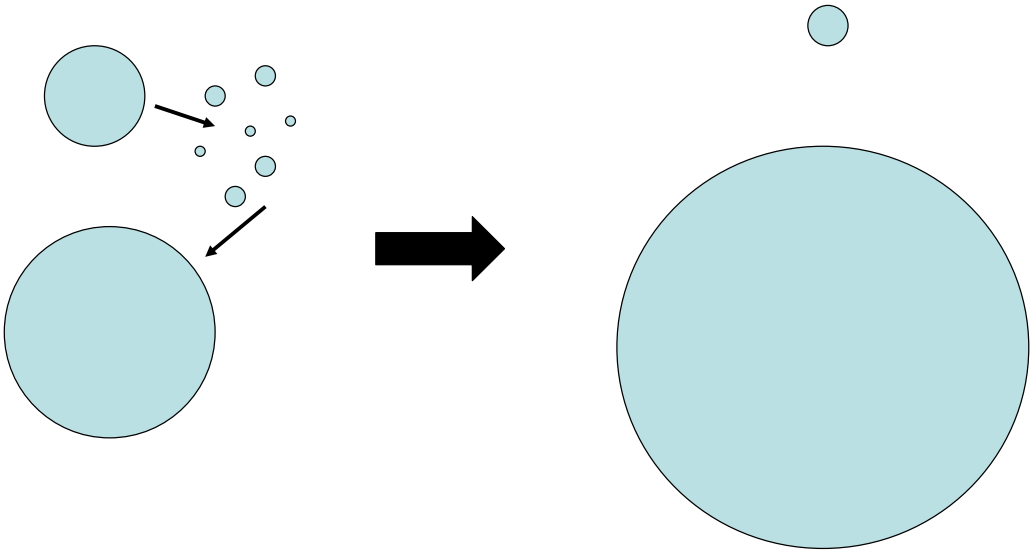

Figure 4.1 Basic process of Ostwald ripening [105].

The energetic stability of the molecules on the surface of a particle is less than the ones in the interior. Thus, the energetically favorable character of larger particles over smaller particles is the reason why thermodynamically-driven spontaneous

process occurs [107]. The free atoms tend to condense on the surface of larger particles when the free atoms in solution are supersaturated [107]. As a result, the average size will incline due to the growing rate of all the lager particles is faster than the shrinking rate of the smaller particles. The entire group of particles will come into one huge spherical particle after an infinite amount of time so that the total surface area will be minimized. Normally, flocculation is found in oil-in-water emulsions ripening while Ostwald ripening is found in water-in-oil emulsions [108].

In order to decrease the overall energy of the system, molecules on the surface of a small particle, which is energetically unfavorable with less than 5 bonded neighbors, will have a tendency to apart from the particle and spread into the solution. The concentration of free atoms in solution goes up when all small particles do follow this step. In some chemical process, the smaller crystals act as the fuel for the growth of larger crystals. In modern technology, Ostwald ripening is the fundamental principle for the solution synthesis of quantum dots [108].

4.1.4 Salts

The Crystal faces with high surface energies, which show the fastest rate of growth, are minimized or even disappear in the final morphology [109]. Wulff's rule illustrates the equilibrium morphology of a crystal which is given by the smallest surface energy of all exposed crystal faces. However, growth of one dimensional nanostructures is generally an unbalanced process that is manipulated by kinetics. Thus a solid foundation of the complex growth kinetics is required for the

controlling of growth process [101]. The shape, size and crystallinity of the products as well as the growth rate are affected by lots of preparation conditions, which including salt's type, the precursor composition, the initial particle size and also the solubility of the precursor constituents in the salt [110]. In hydrothermal synthesis, the precursor, the solvent and maybe the surfactant in some cases are mixed and heated in a closed container, in which the increased temperature also makes the inside pressure go up. Therefore, the solubility and the reactivity of reactants will and enable crystallization nanostructures at a pretty lower temperature than applying other methods [111]. There are various salts can be used in the molten salt synthesis, for instance: chlorides, nitrates and hydroxides. In this project, Sodium Chloride (NaCl) is selected.

4.1.5 Surfactants

Normally, the choice of a surfactant in a synthesis is often randomly due to the knowledge of how strongly certain kinds of surfactants adsorb on specific crystal faces is lacking. The sizes and morphologies of the nanocryatals could be controlled by carefully selecting of the kind of surfactant and its concentration. The factors, which play important parts in the interaction of the surfactant with the material and the solvent are shown as follows:

1. The type: anionic, cationic and non-ionic;
2. The size: length of alkyl chain, polymeric and non-polymeric;
3. The head size: size of polar end;
4. The shape of the nonpolar end: single or double alkyl chain, straight or branched

alkyl chain and benzene rings.

Authors propose Triton X-100 (non-ionic) and Tween 20 (non-ionic) in this project, the detailed working mechanism of them will be discussed in the next chapter.

4.2 Crystallization

Crystallization is a chemical solid–liquid separation technique. Mass transfer of a solute from the liquid solution to a pure solid crystalline phase occurs in crystallization. Thus, crystallization is an aspect of precipitation, as compared to precipitation due to chemical reaction, it is obtained through a variation of the solubility related to the solute in the solvent. Crystallization is the process of natural or artificial, which forms solid crystals precipitating from a solution, melt or more rarely deposited directly from a gas. In chemical engineering, crystallization usually occurs in a crystallizer.

4.2.1 Process

Nucleation is the step where the solute molecules dispersed in the solvent start to gather into clusters, it become stable under the current operating conditions on the nanometer scale. The nucleation is constituted by these stable clusters. However, they will redissolve in the solvent when the clusters are not stable. In order to make the nuclei be stable, the clusters need to reach a critical size, which is dictated by the operating conditions (temperature and supersaturation). At the stage of nucleation, the atoms arrange in a defined and periodic manner that defines the crystal structure , called "crystal structure", which is a special term that refers to

the relative arrangement of the atoms. Even though those are a result of the internal crystal structure, they are not the macroscopic properties of the crystal (size and shape). Nucleation and crystal growth are the two major events consisted in the crystallization process, nucleation is followed by the crystal growth, which succeed in producing the critical cluster size. Since the rate of nucleation and growth is driven by the existing supersaturation in the solution, it is clear that supersaturation is the driving force of the crystallization. The initial nucleation step and the following crystal growth is driven by supersaturation, both of them could not take place in saturated and undersaturated conditions. The crystallization will be completed once the supersaturation is exhausted and equilibrium will be reached by the solid–liquid system, unless the operating conditions are modified from equilibrium, which will supersaturate the solution again. Therefore, nucleation and growth continue to take place simultaneously when the supersaturation exists. Supersaturation is a fundamental factor in crystallization dynamics, which illustrates the difference between the actual value of the solute concentration at the crystallization limit and the theoretical solubility threshold. Based on the different conditions, the predomination of either nucleation or growth over the other enable us to fabricate crystals with different sizes and shapes. Snowflakes are well-known examples, they form in a wide range of complicated shapes. Since the crystals experience many conditions change (for example: temperature and humidity) during its fall to earth [112], it is almost impossible for any two snowflakes to be exactly the same in shape. Different geometries will be obtained due to subtle differences in *crystal growth* conditions. Figure 4.2 shows the pictures of some

different snowflakes, which were took by Wilson Bentley circa 1902.

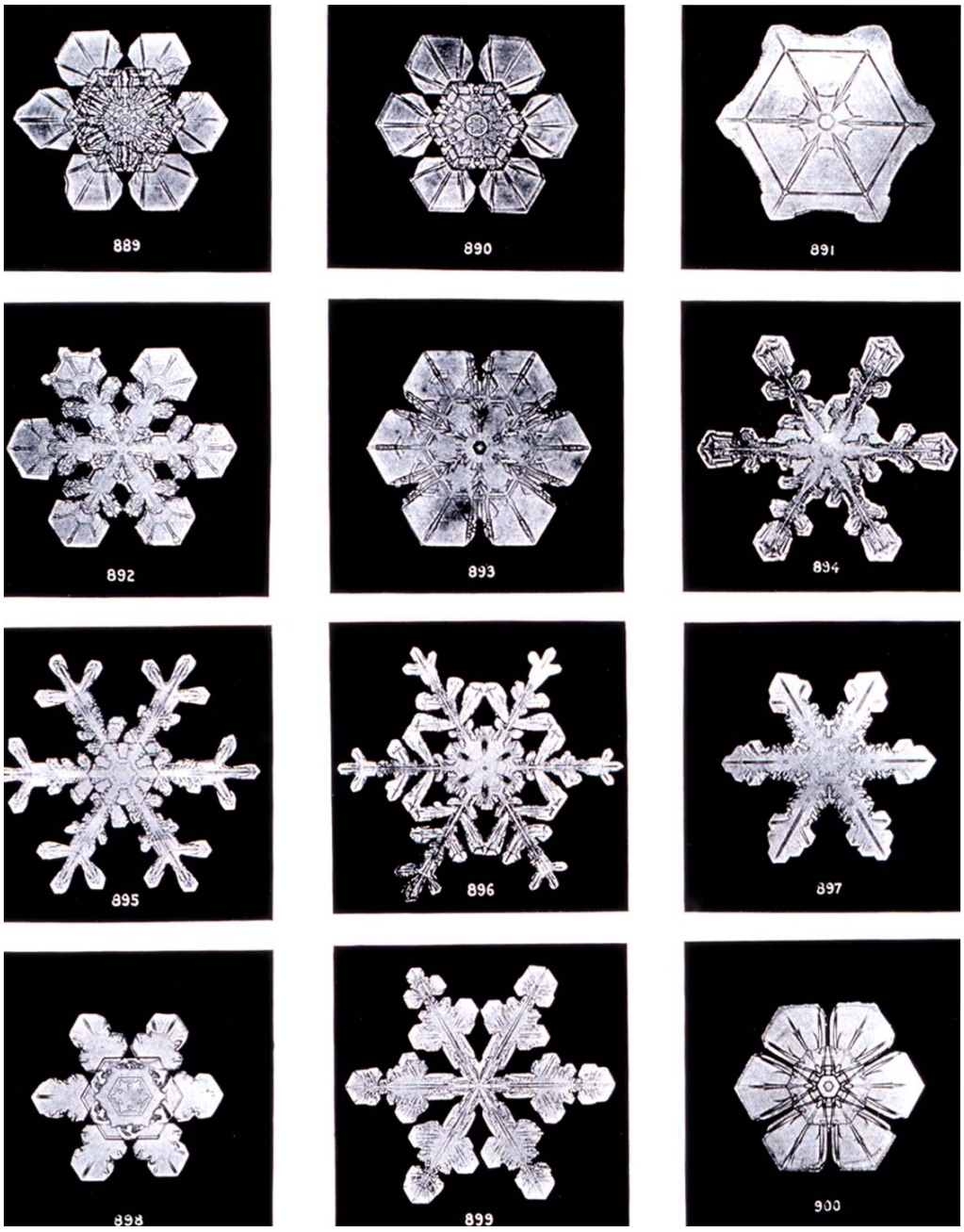

Figure 4.2 Different shapes of snowflakes [112].

In contrast to the classic crystallization, there are some examples of an alternative crystallization mechanism named oriented attachment or mesocrystal formation, which is based on self-assembly [109, 113]. In this specific mechanism, they can

form a mesocrystal through mesoscale assembly if the nanoparticles are coated by adsorbed surfactants, which maybe followed by fusion to a crystal with the same orientation and to a single crystal in the end [109, 113]. Furthermore, primary nanoparticles can be arranged into an iso-oriented crystal through oriented attachment and then grow a single crystal upon fusion of the nanoparticles. As a result, the total energy is declined due to the removal of solid/liquid or solid/gas interface while entropy is increased due to desorption of surfactant [114]. There is a phenomenon called polymorphism, which demonstrates that lots of compounds have the ability to crystallize with different crystal structures. Polymorphism is very important in industrial manufacture of crystalline products, because the crystal polymorphs of the same compound may exhibit different physical properties, for instance: dissolution rate, shape, melting point and so on. Basically, each polymorph is a different thermodynamic solid state.

4.2.2 Dynamics of Crystallization

It is impossible for the solid formation below the solubility threshold at a given temperature and pressure conditions, may then occur at a concentration much higher than the theoretical solubility level. A crystal is formed by following a well-defined pattern and driven by forces acting at the molecular level. As a result, the crystal is in an environment where the solute concentration reaches a specific critical value during the process of formation.

Crystal size distribution

In crystallization, the appearance and size range of a crystalline product are in the

most imperative place. It is an important fact that larger crystals have a much smaller surface area to volume ratio than small particles, which results in a higher purity. Furthermore, large crystals are much easier to filter out of a solution than small crystals. Large crystals with uniform size are essential for washing, filtering, transportation, and storage if further processing of the crystals is wanted. A relatively complicated mathematical process called population balance theory is able to estimate the theoretical crystal size distribution as a function of operating conditions. Because of the less retention of mother liquor which includes impurities and a smaller loss of yield when the crystals are washed to get rid of the mother liquor, we can get a higher purity.

Crystal growth

The original nucleus that may capture in a time unit is called the growth rate, which can be expressed as kg/(m^2*h), is a constant specific to the process. The nucleus acts as a convergence point for molecules of solute touching or adjacent to the crystal so that it can develop its own dimension in successive layers. Many physical factors have influence on the growth rate, for example: pressure, temperature, Reynolds number, and so on.

Here are the main values need to be controlled:

1. Flow pattern: an index of the possibility of a molecule of solute to contact with an existing crystal (in laminar flow: higher, in turbulent flow: lower, but the inverse applies to the possibility of contact).

2. Supersaturation value: an index of the amount of solute available for the growth of the crystal;

3. Retention time: an index of the probability of a molecule of solute to contact with an existing crystal;

4. Total crystal surface per unit fluid mass: an index of the ability of the solute to fix onto the crystal;

Nucleation

Nucleation is a result of rapid local fluctuations on a molecular scale in a homogeneous phase, which is in the state of metastable equilibrium. It is defined as a phase change in a small region, like the formation of a solid crystal from a liquid solution. Total nucleation is the sum effect of primary nucleation and secondary nucleation.

Primary nucleation

Two conditions may result in the primary nucleation. The first one is homogeneous nucleation that is not influenced in any way by solids, in which solids contain the walls of the crystallizer vessel and particles of any foreign substance. The second one is heterogeneous nucleation, which occurs when solid particles of foreign substances cause an incline in the rate of nucleation that would not be seen without the existence of foreign particles. Primary nucleation, both of the homogeneous and heterogeneous, has been modelled as follows [115]:

$$B = \frac{dN}{dt} = k_n(c - c^*)^n$$

$(c–c^*)$: supersaturation.

c: the instantaneous solute concentration.

c^* : the solute concentration at saturation.

k_n: rate constant.

n: empirical exponent that can be as large as 10, generally ranges from 3 to 4.

N: the number of nuclei per unit volume.

B: the number of nuclei formed per unit volume per unit time.

Primary nucleation is the initial formation of a crystal where no other crystals present, or where if crystals present in the system but do not have any influence on the process. Since the high energy necessary to begin nucleation without a solid surface to catalyse the nucleation, homogeneous nucleation seldom happens in practice.

Secondary nucleation

Fluid shear is the cause of the first type of known secondary crystallization, the other one attributable to collisions between existing crystals with a solid surface of the crystallizer or other crystals themselves. Fluid shear nucleation usually takes place when liquid travels across a crystal at a high speed, getting rid of nuclei which would be incorporated into a crystal, making the swept-away nuclei to become new crystals. Secondary nucleation is the formation of nuclei due to the impact of the existing microscopic crystals in the magma [116]. The following model is often used to model secondary nucleation [115]:

$$B = \frac{dN}{dt} = k_1 M_T^j (c - c^*)^b$$

$(c–c^*)$: supersaturation.

c: the instantaneous solute concentration.

c^* : the solute concentration at saturation.

N: the number of nuclei per unit volume.

B: an empirical exponent that goes up to 5, but is 2 in general.

J: an empirical exponent that goes up to 1.5, but is 1 in general.

M_T: the suspension density.

k_1: a rate constant.

The most effective and common method for nucleation is the contact nucleation, which has the benefits shown as follows [116]:

1. Low energy required at which crystals strike stops the breaking of existing crystals into new crystals.

2. Low kinetic order and proportional to supersaturation, which allows easy control without unstable operation.

3. The quantitative fundamentals have been isolated and are going to be incorporated into practice.

4. Takes place at low supersaturation, where growth rate is optimum for good quality.

4.2.3 View from Thermodynamics

There are some factors can have a major influence on the size, number, and shape of the produced crystals, for instance: impurity level, mixing regime, vessel design, and cooling profile. At some sharply defined temperature, the complicated architecture of the crystal collapses to liquid. Generally, thermodynamic and kinetic factors are able to govern the nature of a crystallization process, which make it pretty variable and difficult to control.

Thermodynamics from textbook says that melting occurs due to the entropy, *S*, develop your system by spatial randomization of the molecules has overcome the enthalpy, *H*, loss as a result of breaking the crystal packing forces:

$$T(S_{liquid} - S_{solid}) > H_{liquid} - H_{solid}$$

$$G_{liquid} < G_{solid}$$

When the temperature is increasing, this rule suffers no exception. The ordering of molecules within the system is overcompensated by the thermal randomization of the surroundings result in the decreasing of entropy. For the same reason, at the same temperature the molecules should transfer into the very same crystalline form. The entropy goes down because of the ordering of molecules within the system is overcompensated by the thermal randomization of the surroundings. On the other hand, the entropy of the universe goes up due to the release of the fusion's heat.

However, liquids which behave in this way on cooling are the exception over the rule. The nucleation and growth of a crystal are under kinetic instead of thermodynamic control. It is much easier for us to dissolve crystal into solvent than to grow the resulting solution back to perfect crystal. Despite of the second principle of thermodynamics, crystallization normally happens at lower temperatures, which means that a crystal is more easily to be destroyed than it is formed.

4.2.4 Artificial Techniques

A solution must be supersaturated to make crystallization occur, which means that

the solution has to contain more solute molecules or ions dissolved than it would originally contain under the equilibrium (saturated solution). The methods can be used to achieve this are showed as follows:

● Changing in pH (the most common methods used in industrial practice);

● Chemical reaction;

● Adding a second solvent to reduce the solubility of the solute, methods known as antisolvent or drown-out;

● Solvent evaporation;

● Solution cooling.

Equipments

Tank crystallizer is the most typical equipment. In tank crystallization, saturated solutions are allowed to be cooled in open tanks. It is a quite old method which is still used in some specialized cases. The mother liquid will be drained and the crystals will be removed after a period of time, but the nucleation and size of crystals are difficult to control. On the other hand, labor costs are very expensive.

Purification

Purification is the method widely used to improve (obtaining very pure substance) and verify their purity. Since each molecule or ion must fit perfectly into the lattice as it leaves the solution, well formed crystals are expected to be pure. A product from a liquid feedstream is separated by crystallization, mostly in extremely pure form. In order to form crystals, cooling the feedstream or adding precipitants which lower the solubility of the desired product. Molecular recognition is regarded as the principle of purification in crystallization because of the impurities would normally

not fit as well in the lattice and remain in solution preferentially. However, there are examples when impurities incorporate into the lattice, which in result of decreasing the level of purity of the final crystal product. In some other cases, the solvent may be 'trapped' in liquid state within the crystal formed which is known as inclusion. Furthermore, a solvate is formed by incorporate the solvent into the lattice forming.

Crystal Fabrication

A perspective from material industry :

1. Very small size crystals: Thin film production.

Powder, sand and smaller sizes: using methods for powder and controlled forms.

a. Sample production: small production of very small crystals for material characterization. In order to determine the structures of an immense variety of molecules, including inorganic compounds and bio-macromolecules, techniques like X-ray crystallography and NMR spectroscopy have been widely used in chemistry and biochemistry. Controlled recrystallization is an imperative method to supply unusual crystals, which are essential to display the molecular structure and nuclear forces inside a typical molecule of a crystal.

b. Mass-production: salt-powder production (chemical industry).

2. Macroscopic crystal production: to supply the demand of natural-like crystals with some methods which are "accelerate time-scale" for massive production and perfection: Ionic crystal production and covalent crystal production.

4.3 Single Crystal

In single crystal or monocrystalline solid, the crystal lattice of the whole sample is

continuous to the edges of the sample with no grain boundaries. Since entropic effects are in favor of some imperfections in the microstructure of solids, for instance: impurities, inhomogeneous strain and crystallographic defects, perfect single crystals with meaningful size are extremely rare in nature. Depending on the type of crystallographic structure, the absence of the defects with grain boundaries is able to give monocrystals unique properties in the areas of mechanical, optical, electrical and anisotropic. In the area of technological applications, especially in electronics and optics, these properties are widely used.

Polycrystalline exists in between of the single crystal and its opposite side. It is made up of lots of smaller crystals which are known as crystallites and paracrystalline phases. An amorphous structure, where the atomic position is limited to short range order, is the opposite side of single crystal. Imperfect single crystals are capable to reach huge sizes in nature, for example: several mineral species (beryl, gypsum and feldspars) are recognized to have produced crystals several meters across. Even though they can be made under controlled conditions, perfect single crystals with perfect sizes are also very difficult to fabricate in the lab.

4.3.1 Manufacture

Depending on the physical properties of the substance, some specific methods of crystallization with less exotic also may be used, for instance: hydrothermal synthesis, sublimation, or simply solvent based crystallization. In fabrication of

silicon and metal single crystal, the techniques used involve relatively slow and highly controlled crystallization. There are some other techniques to produce large single crystals, such as the Czochralski process and the Bridgman technique. There is another different technology to create single crystalline materials which is called epitaxy. It has many potential applications in other nanoscale technological fields and catalysis, it is also used to deposit very thin (scale: from micrometer to nanometer) layers of materials onto the surface of an existing single crystal, which has lots of applications in the areas of semiconductor production.

4.3.2 Applications

Materials engineering

Turbine blade is an application of single crystals in the production of high strength materials with low thermal creep [117]. The short of grain boundaries decreases the amount of creep which is important for high temperature, high tolerance applications.

In research

Single crystals are essential in research, especially for the areas of Condensed Matter Physics, Materials science and so forth. It is possible for us to study directional dependence of different properties only in single crystals. The detailed study of a material's crystal structure by the techniques like Bragg diffraction and helium atom scattering, go much easier with monocrystals. In superconductivity, some cases show that superconductivity can be only seen in

single crystalline specimen.

Electrical conductors

Even though no single crystal copper is produced on a large scale industrially before, many methods of producing large individual crystal sizes for copper conductors are being used for high performance electrical applications. Generally, single crystal copper owns higher conductivity than polycrystalline copper [118].

Semiconductor industry

Single crystal silicon is typically used in the synthesis of semiconductors. Microprocessor producers have made a heavy investment the production of large single crystals of silicon. On the quantum scale where microprocessors run, grain boundaries would have a big influence on the functionality of field effect transistors by changing local electrical properties.

4.4 Synthesis of single-crystalline PZT nanorods

4.4.1 Experiments

The formation of nanorods was done by using a surfactant-salt-assisted process. More specifically, the obtained PZT crystals and NaCl were mixed together and crashed for 30 minutes. In succession, they were added into the liquid surfactant Triton and the molar ratio of PZT: NaCl: Triton was 1: 5: 10. The mixture was then sonicated in the water bath for 15 minutes before being preheated at 110 degree for 1 hour. After preheating, the obtained starting materials were sintered at 300°C for 2 hours and afterwards increased to 800°C with a ramping rate of approximately

8°C/min for annealing 3 hours in the open air. Finally, the products were washed by distilled water for 5 times to get rid of NaCl and dried at 60°C for 4 hours. Figure 3.1 shows the steps of fabricating PZT-nanorods. Figure 4.3 describes the process of synthesizing PZT nanocrystals

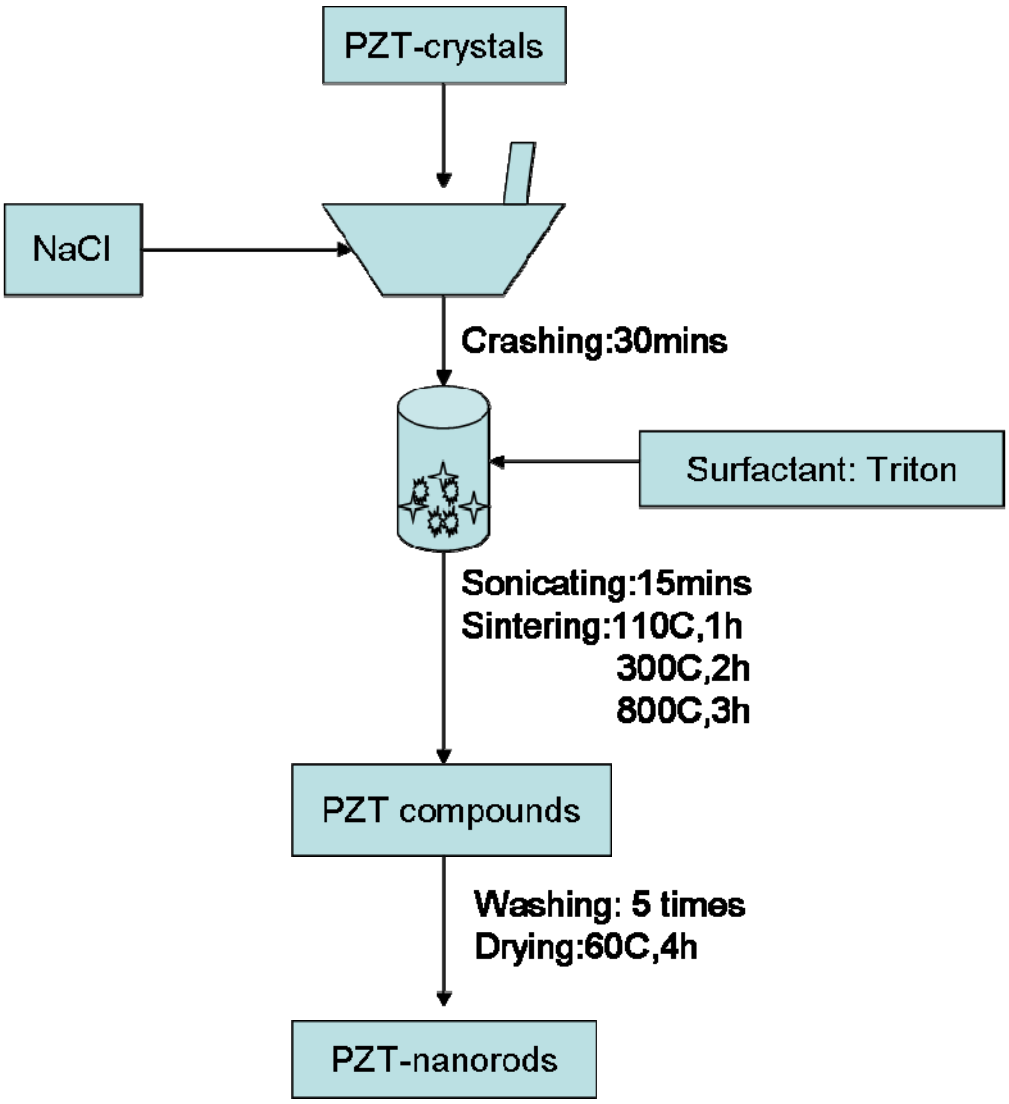

Figure 4.3 Process of synthesizing PZT-nanorods

4.4.2 Results

Some of the PZT nanocrystals and PZT nanorods were carefully selected and

analyzed by X-ray diffraction (XRD) to verify the crystal structures and phases. A Raman scattering spectrometer was brought out for characterizing the structures. The morphology of the nanorods was investigated by Scanning Electron Microscopy respectively. Selected area electron diffraction (SAED) and high resolution transmission electron microscopy (HRTEM) were also used to test the sample.

Effect of reaction time on the product

The as-prepared PZT nanocrystals were then mixed with Triton and NaCl to fabricate PZT nanorods. The XRD spectrums of the PZT-Triton, PZT-Triton sintered at different times are shown in Figure 4.4a. The sintering temperature was set at 800°C, three different sintering times have been tried to investigate the effect of reaction time. Comparing the patterns of PZT-Triton sintered at 3h, 4h30min and 6h, the perovskite peaks of PZT-Triton shifted slightly with prolonging the sintering time, which shows a reduction of Zr in the sample and the molar ratio of Pb: Zr: Ti was no longer at the morphotropic phase boundary. As a result, nanorods only appear when the sintering condition was set for 3 hours and 800°C.

As the labeled peaks in Figure 4.4a, there are three different phases in this product: triclinic $Pb(Zr_{0.52}Ti_{0.48})O_3$ (PDF No. 97-024-6572), monoclinic $Pb(Zr_{0.53}Ti_{0.47})O_3$ (PDF No. 97-009-7063) and orthorhombic ZrO_2(97-006-7004). A comparison between the PZT nanorods and PZT nanocrystals was made in Fig 4.4b, the one with PZT nanorods owns three different phases while that of PZT nanocrystals only has one single phase.

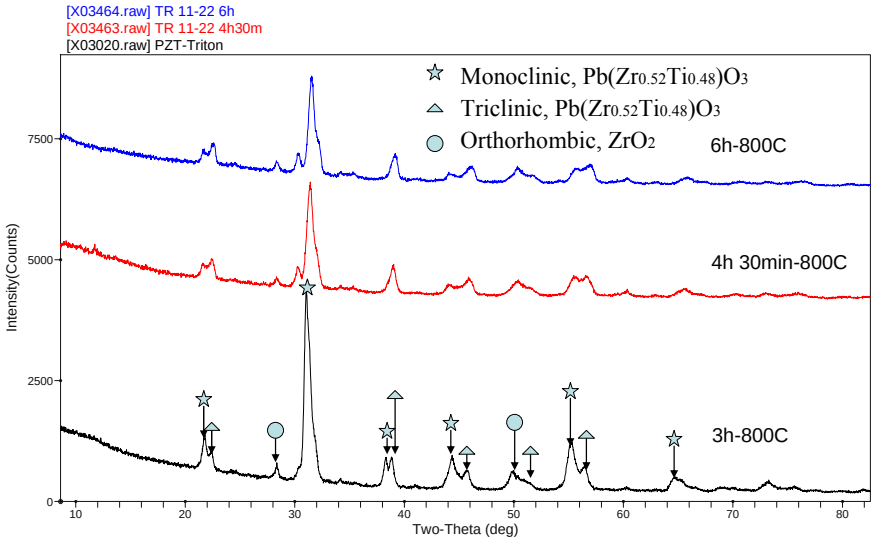

a

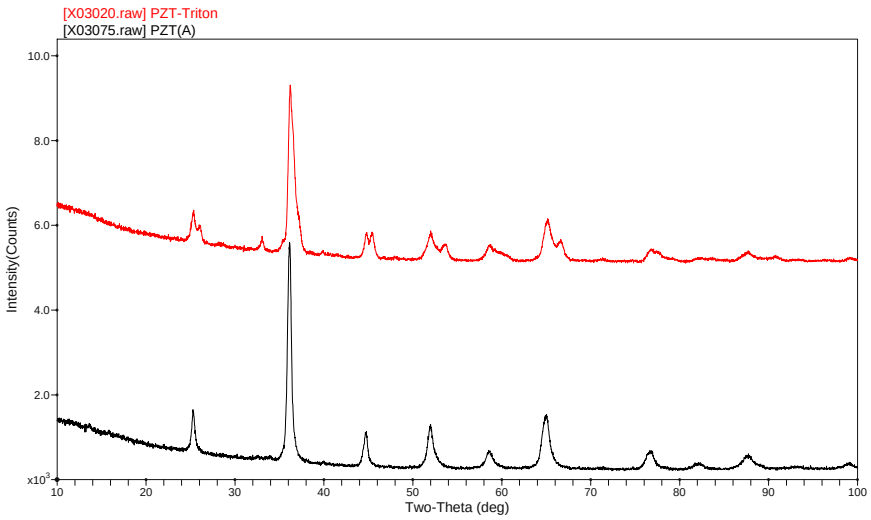

b

Figure 4.4 Typical XRD patterns of a) PZT-Triton at different reaction temperatures. b) PZT nanorods versus PZT nanocrystals

Raman spectra of PZT nanorods

Figure 4.5 shows the Raman spectra of PZT nanorods. The parameters used for the tests were the same as the PZT nanocrystals: 1) Excitation laser wavelength: 780

nm; 2) exposure time: 10sec; 3) Charge Coupled Device (CCD) detector; 4) backscattering geometry. Similar as the PZT nanocrystals, the locations of the Raman shift peaks of PZT nanorods match well with the typical Raman peaks of perovskite PZT [87, 88]. By comparing the Raman spectra of PZT crystals and nanorods, the one of PZT nanorods decreased in intensity. Furthermore, the Raman modes of A_1(2TO), E(2TO) and A_1(3LO) noticeably shift to lower frequencies (192, 314 and 725 cm^{-1}), whereas the mode A_1(3TO) and the silent mode B_1+ET only downshift slightly. The weakening in intensity and downshifting in frequency of the Raman lines can be described as the mode-soften behaviors, which signify there is a phase transition between PZT nanocrystals and PZT nanorods [87].

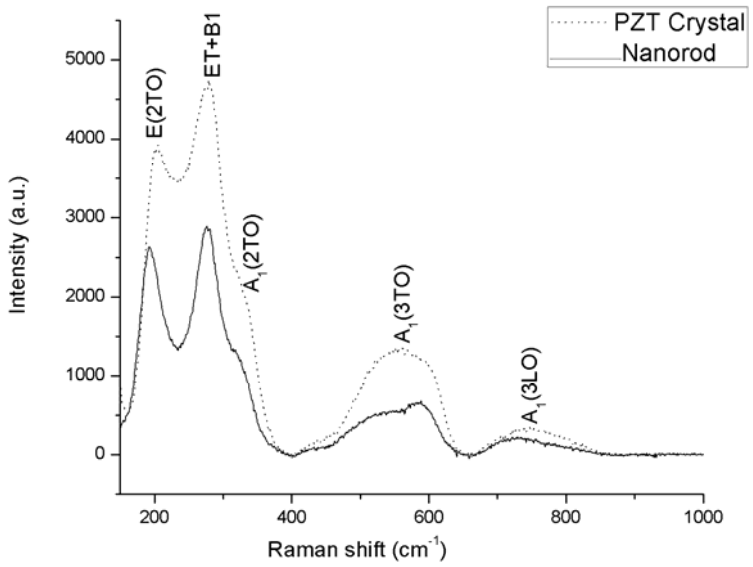

Figure 4.5 Raman Spectra of PZT nanorods versus PZT nanocrystals

SEM investigation of PZT nanorods

Figure 4.6a is a SEM image of PZT nanorods while Figure 4.6b is a SEM image of a individual PZT nanorod. Clearly, lots of nanorods have been successfully

produced when sintered the PZT-Triton at 800°C for 3 hours. SEM images gave us general ideas of the morphology of PZT nanorods. To get further information about the PZT nanorods, a TEM testing had been utilized for the sample.

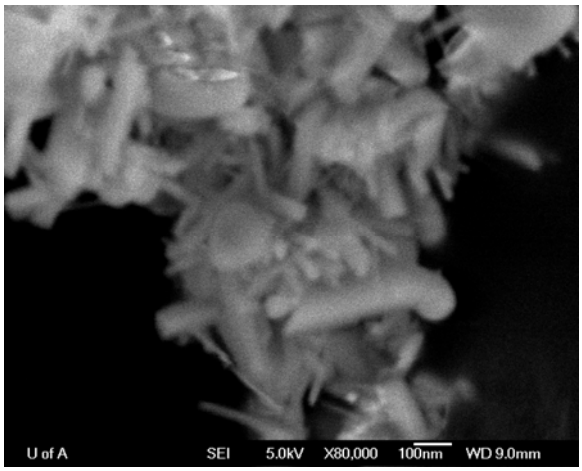

a

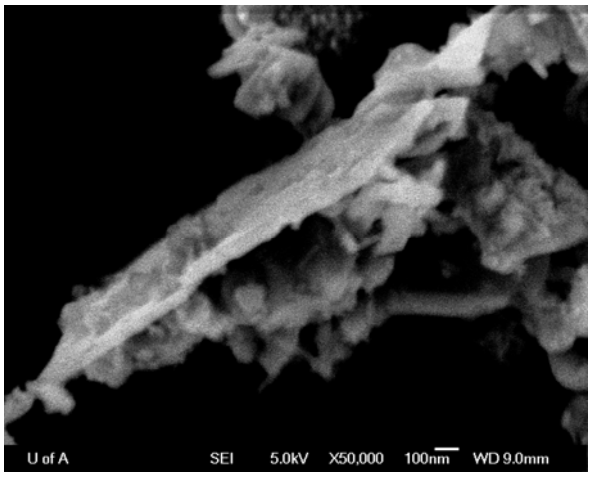

b

Figure 4.6 a) SEM image of PZT nanorods. b) SEM image of a typical PZT nanorod.

TEM investigation of PZT nanorods

Figure 4.7a reveals the morphologies of the PZT nanorods prepared by Triton. Figure 4.7b is a typical TEM image of an individual PZT nanorod, illustrating that

the nanoscale PZT rods, with diameters around 70-130 nm and lengths over 1 um, have been indeed fabricated.

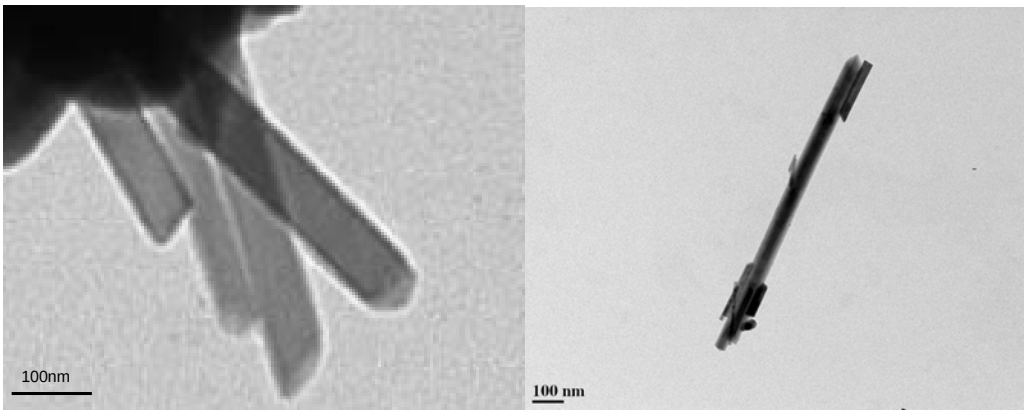

a b

Figure 4.7 a) TEM image of PZT nanorods. b) TEM image of a typical PZT nanorod.

Figure 4.8a shows the High Resolution TEM (HRTEM) image of a single PZT nanorod. In order to investigate the crystal structure of the PZT nanorod, a cubic region of the nanorod was selected. A HRTEM image with high magnification was took in this cubic area, and Nano Beam Diffraction (NBD) Pattern of the corresponding area is shown in Figure 4.8b. As can be seen, a well organized spots-pattern instead of diffraction rings is represented in the NBD pattern of the PZT nanorods, declaring that the nanorod is single crystal. The clear lattice fringes in the enlarged cubic area demonstrate the single crystalline structure of the PZT nanorod.

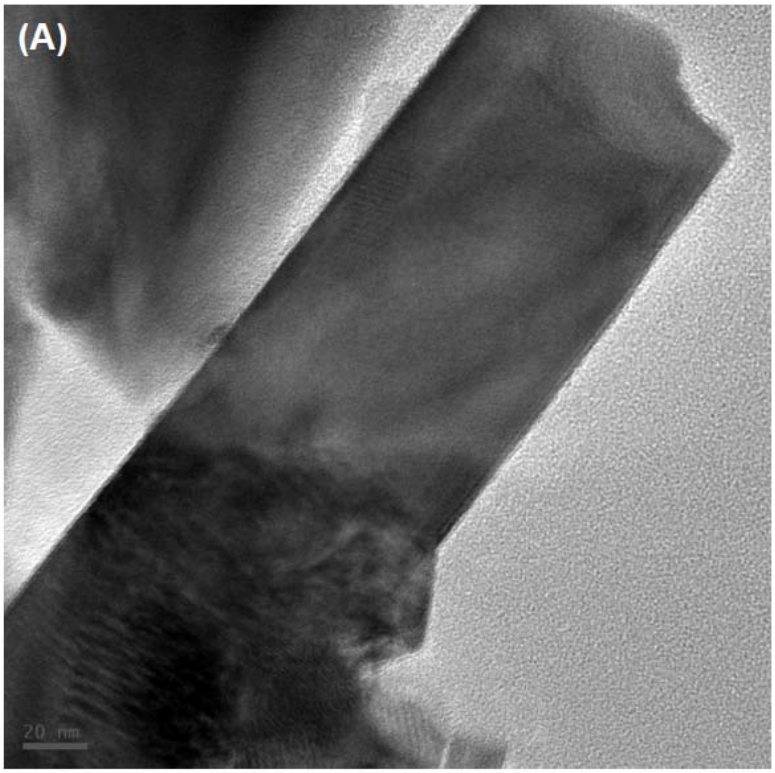

HRTEM image of one nano rod in sample PZT triton

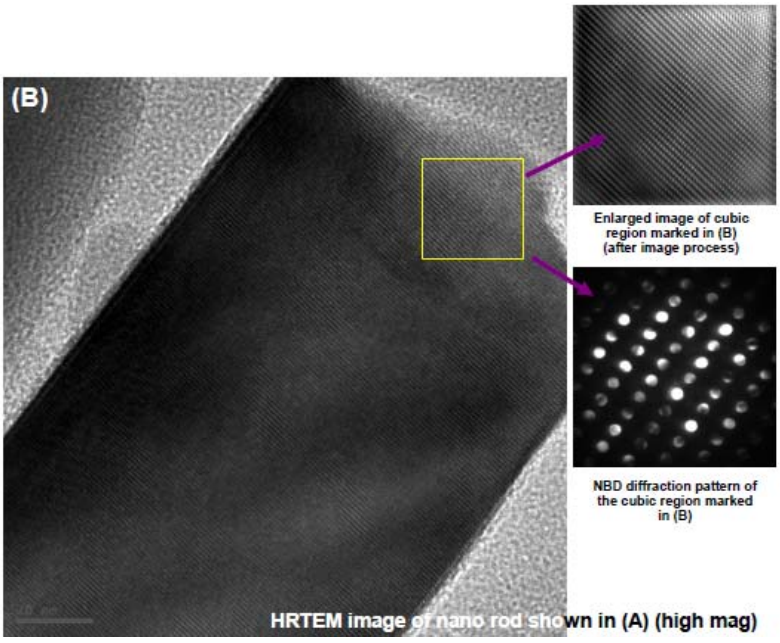

Figure 4.8 a) High-resolution TEM image of a typical PZT nanorod. b) High-resolution TEM image of an individual PZT nanorod and its corresponding Nano Beam diffraction (NBD) pattern.

4.5 Synthesis of single-crystalline PZT nanohexagons

4.5.1 Experiments

The formation of nanohexagons was done by using a surfactant-salt-assisted process and the steps are displayed in Figure 4.9. More specifically, the obtained PZT crystals and NaCl were mixed together and crashed for 30 minutes. In succession, they were added into the liquid surfactant Tween 20 and the mass ratio of PZT: NaCl: Tween 20 was 1: 5: 10. The mixture was then sonicated in the water bath for 15 minutes before being preheated at 110 degree for 1 hour. After preheating, the obtained starting materials were sintered at 300°C for 2 hours and afterwards increased to 800°C with a ramping rate of approximately 8°C/min for annealing 3 hours in the open air. Finally, the products were washed by distilled water for 5 times to get rid of NaCl and dried at 60°C for 4 hours.

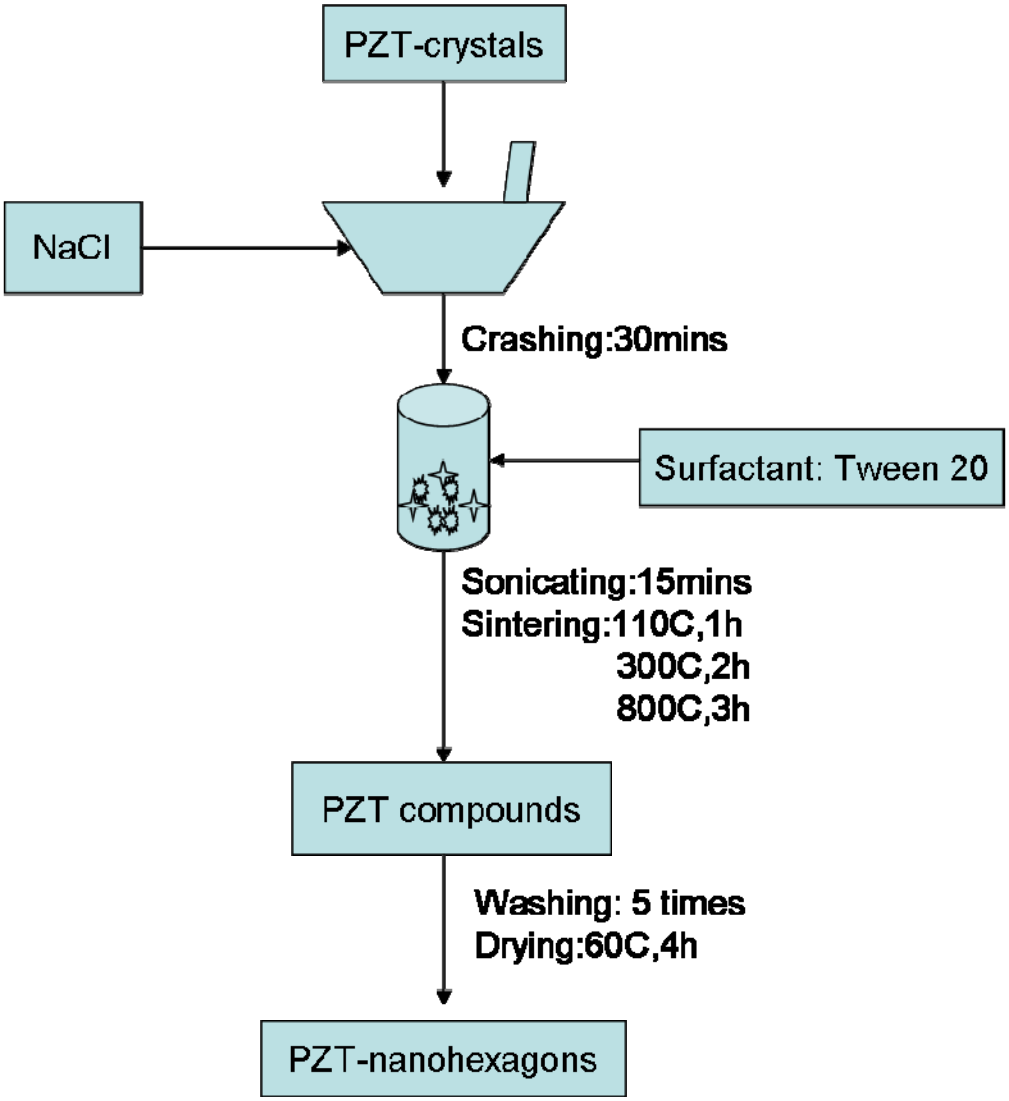

Figure 4.9 Process of fabricating PZT nanohexagons

4.5.2 Results

Some of the PZT nanocrystals and PZT nanohexagons were carefully selected and analyzed by X-ray diffraction (XRD) to verify the crystal structures and phases. A Raman scattering spectrometer was brought out for characterizing the structures. The morphology and selected area electron diffraction (SAED) were investigated by a transmission electron microscopy (TEM) and high resolution TEM (HRTEM).

Effect of reaction time and temperature on the product

The prepared PZT nanocrystals were then mixed with Tween 20 and NaCl to fabricate PZT nanohexagons. The XRD spectrums of the PZT-Tween 20, PZT-Tween 20 sintered at different temperatures and times are shown in Figure 4.10a and Figure 4.10b, respectively. The effect of reaction temperature on the product was investigated by sintering the PZT-Tween 20 for 3 hours at 750°C, 800°C and 850°C respectively, and the results are shown in Fig 4.10a. Even though the intensities of each XRD pattern does not show clear difference, only the PZT-Tween 20 sintered at 800°C for 3 hours gave us PZT nanohexagons (further confirmed by TEM). As the labeled peaks in Figure 4.10a, there are three different phases in this product: triclinic $Pb(Zr_{0.52}Ti_{0.48})O_3$ (PDF No. 97-024-6572), monoclinic $Pb(Zr_{0.53}Ti_{0.47})O_3$ (PDF No. 97-009-7063) and orthorhombic ZrO_2 (97-006-7004). The detailed information about the crystal phase will be confirmed in the future. After setting the sintering temperature at 800°C, 5 different sintering times have been tried to investigate the effect of reaction time. Comparing the patterns of PZT-Tween 20 sintered at 2h30min, 3h, 3h30min, 4h30min and 6h, the perovskite peaks of PZT-Tween 20 became sharper slightly with prolonging the sintering time, which indicative of higher extent of crystallinity and larger grain size [119, 120, 121]. However, nanohexagons only appear when sintering PZT-Tween 20 for 3 hours at 800°C.

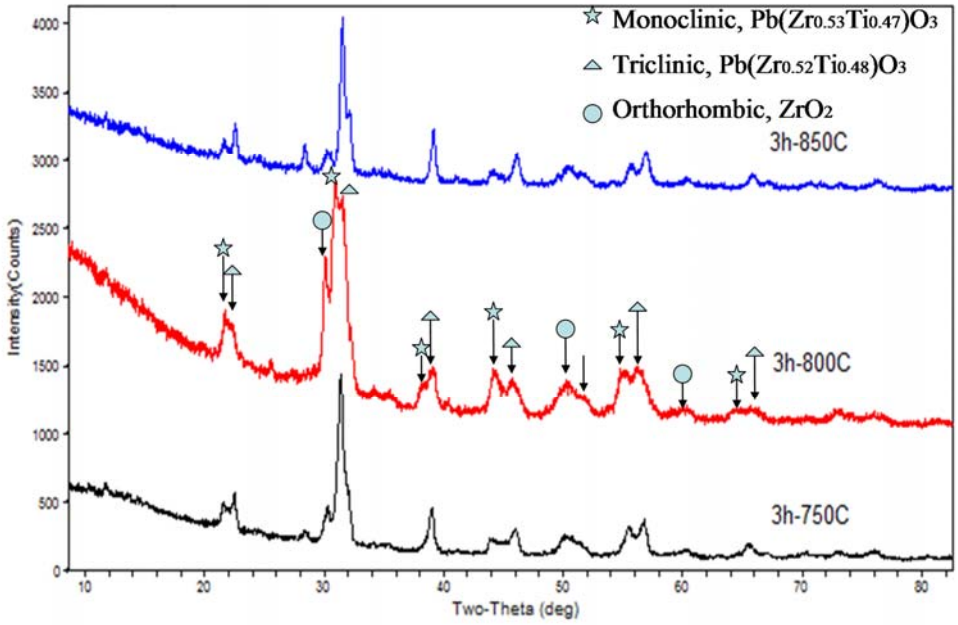

a

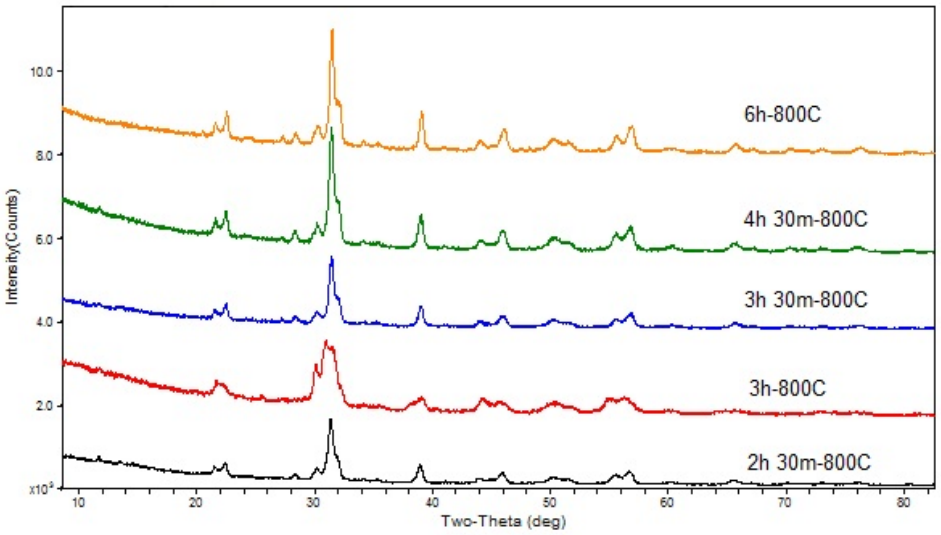

b

Figure 4.10 Typical XRD patterns of a) PZT-Tween 20 at different reaction temperatures. b) PZT-Tween 20 at different reaction times.

Figure 4.11 displays the transmission electron microscopy(TEM) images of PZT-Tween 20 sintered at 5 different conditions: 3 hours at 750°C, 3 hours at 800°C, 3 hours at 850°C, 2 hours 30 mins at 800°C and 3 hours 30 mins at 800°C. As can be seen, only the PZT-Tween 20 sintered at 800°C for 3 hours shows hexagon shape.

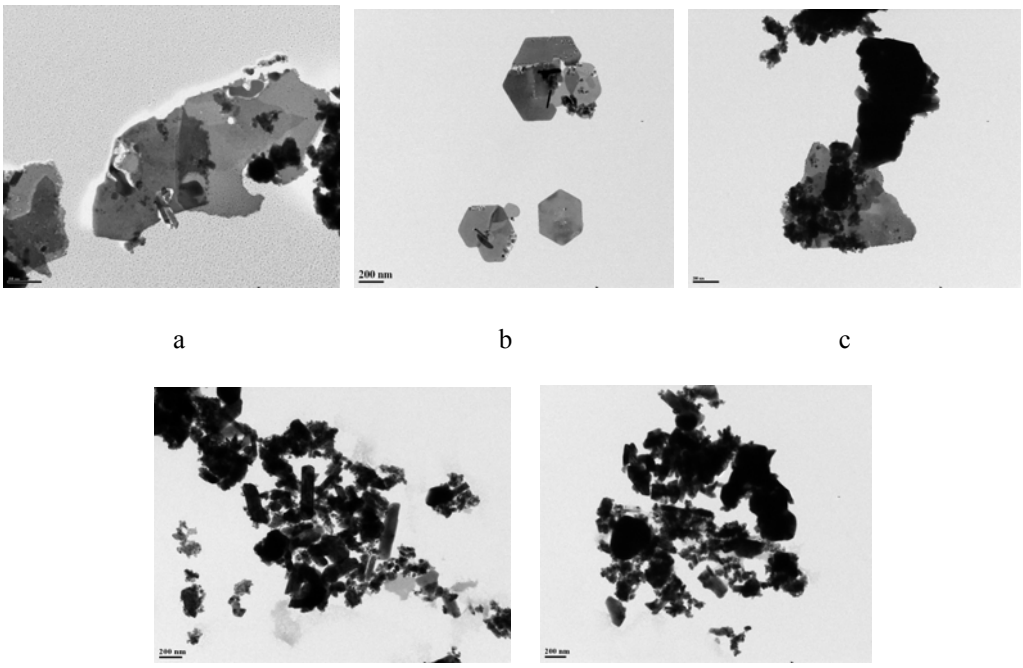

Figure 4.11 TEM images of PZT-Tween 20 sintered at a) 800°C for 2 hours 30 mins. b) 800°C for 3 hours. c) 800°C for 3 hours 30 mins. d) 750°C for 3 hours. e) 850°C for 3 hours.

Raman spectra of PZT nanohexagons

Figure 4.12 shows the Raman spectra of PZT nanohexagons. The parameters used for the tests were the same as the PZT nanocrystals and PZT nanorods: 1) Excitation laser wavelength: 780 nm; 2) exposure time: 10sec; 3) Charge Coupled Device (CCD) detector; 4) backscattering geometry. Similar as the PZT

nanocrystals and PZT nanorods, the locations of the Raman shift peaks of PZT nanohexagons match well with the typical Raman peaks of perovskite PZT [87, 88]. By comparing the Raman spectra of PZT crystals and nanohexagons, the one of PZT nanohexagons decreased in intensity. Furthermore, the Raman modes of A_1(2TO), E(2TO) and A_1(3LO) noticeably shift to lower frequencies (194, 313 and 723 cm^{-1}) while the mode A_1(3TO) and the silent mode B_1+ET only downshift slightly. The weakening in intensity and downshifting in frequency of the Raman lines can be described as the mode-soften behaviors, which signify there is a phase transition between PZT nanocrystals and PZT nanohexagons [87].

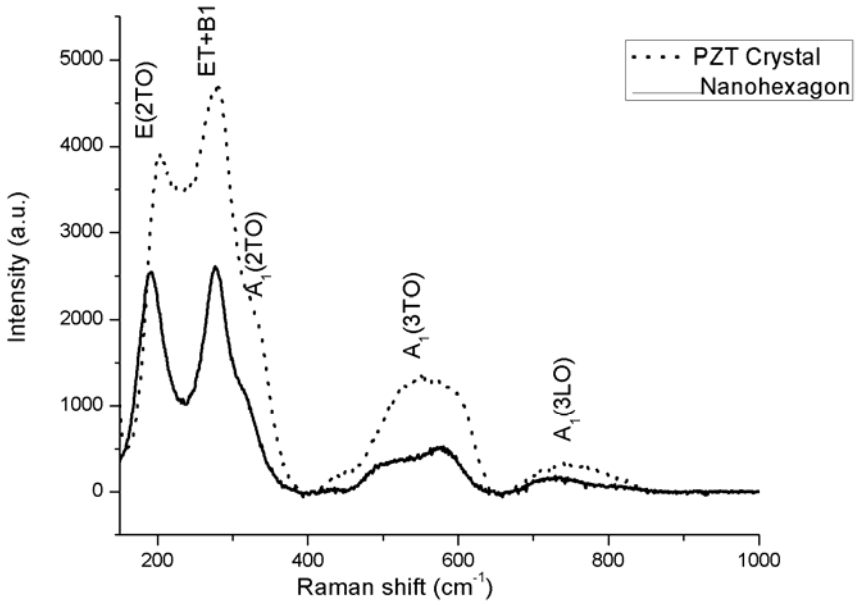

Figure 4.12 Raman spectra of PZT nanohexagons versus PZT nanocrystals.

TEM investigation of PZT nanohexagons

Figure 4.13a shows the shape of the PZT nanohexagons assisted by a liquid

surfactant Tween 20 and NaCl, we can clearly see the hexagon structure of the nanoscale PZT. The PZT nanohexagons, with typical diameters around 480nm-540nm and boundary lengths ranging from 230 to 260nm have been fabricated successfully. A typical TEM picture of an individual PZT nanohexagon was also shown in Figure 4.13b.

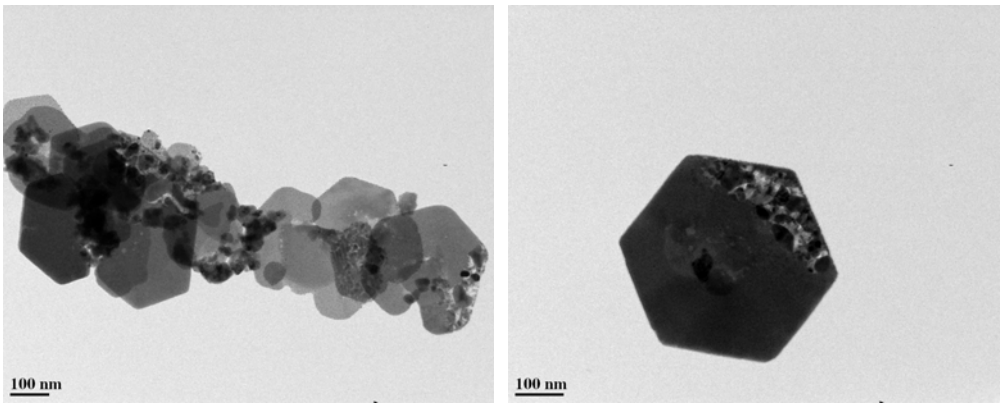

a b

Figure 4.13 a) TEM image of PZT nanohexagons. b) TEM image of an individual PZT nanohexagon.

Figure 4.14 reveals the High Resolution TEM (HRTEM) image of a single PZT nanohexagon. In order to investigate the crystal structure of the PZT nanohexagon, a cubic region of the nanohexagon was selected. A HRTEM image with high magnification was took in this cubic area, and the selected area electron diffraction (SAED) pattern of the corresponding area is shown in this figure. As can be seen, a well organised spots-pattern instead of diffraction rings is represented in the SAED pattern of the PZT nanohexagons, declaring that the nanohexagon is single crystal. Moreover, the SAED patterns got from different areas of the individual hexagon are almost identical. The clear lattice fringes in the enlarged cubic area demonstrate the

single crystalline structure of the PZT nanohexagon, which is in line with the SAED results.

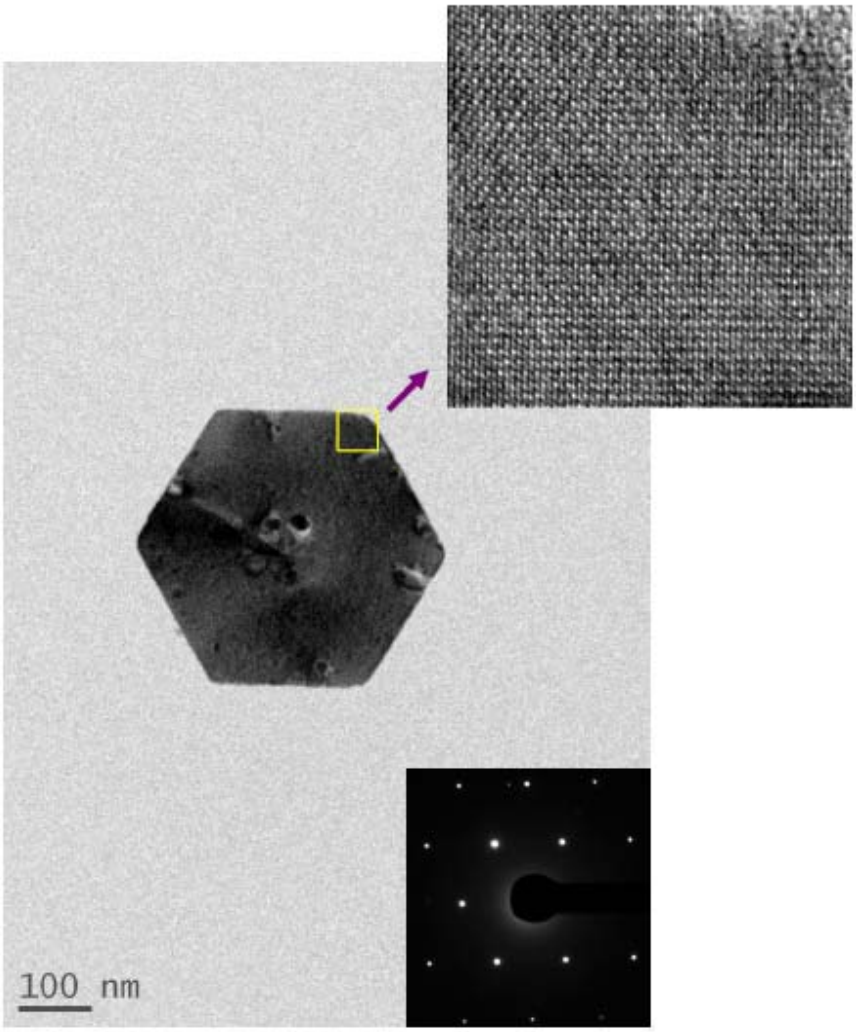

Figure 4.14 High-resolution TEM image of an individual PZT nanohexagon and its corresponding selected area electron diffraction (SAED) pattern.

Chapter 5 Discussion

The necessity of the surfactant is showed and discussed in Chapter 5, the working mechanisms of Triton and Tween 20 are also proposed in 5.2 and 5.3, respectively.

5.1 Influence of the surfactants and NaCl on the formation of PZT nanorods and nanohexagons

In order to identify the influence of the surfactants and NaCl on the formation of PZT nanorods and nanohexagons, one more experiment was carried out: PZT nanoparticles were only mixed with NaCl, no surfactant was assisted. Since the crystals do not grow during the cooling process [122], the cooling rate was not taken into consideration. The product from this experiment was examined by TEM, only irregular-shaped nanoparticles were observed, no nanorods or nanohexagons were found (see Figure 5.1a and Figure 5.1b). Since no particular PZT morphology could be formed in the absence of surfactants, it is believed that the liquid surfactant Triton and Tween 20 played critical roles in the formation of nanorods and nanohexagons, respectively.

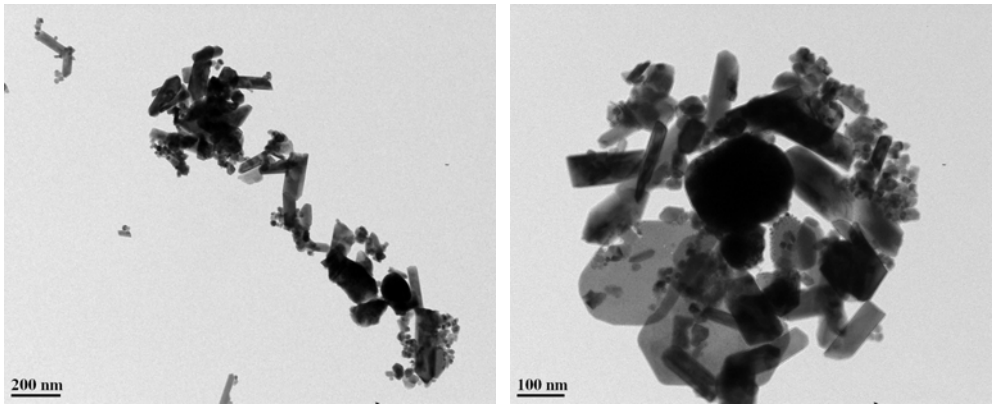

a b

Figure 5.1 TEM images of PZT sintered with NaCl only.

In order to study the synthesis of PZT nanorods and nanohexagons, a clear understanding of the growth mechanism is further required.

5.2 Mechanism of PZT nanorod formation

Here the author proposes that the nanorods produced by our method grow mainly by an Oswald ripening mechanism. Ostwald ripening is an observed phenomenon in solid solutions or liquid sols, reporting the change of an inhomogeneous structure over a period of time. More specifically, small crystals or sol particles dissolve and redeposit onto larger crystals or sol particles over the time [105].

The characters of the starting materials such as chemical activity or size must have great effect on the growth of PZT nanorods, when Ostwald ripening mechanism is in the dominant position [122, 123]. Under the combined effects of NaCl flux and surfactants, the fine powders dispersed and redeposited on larger particles, which

formed the PZT nanorods along an axial direction. The components in the flux could move around more easily due to the viscosity of the melt was effectively decreased by adding NaCl [124]. Thus, the NaCl flux is able to provide a favorable liquid environment for the PZT nanorods growth. As to the surfactant Triton, it prevents the small particles from gathering to large particles by forming a "shell" surrounding the small particles and the nanorod. The triton gradually burns in the sintering process with emitting light smoke. After the Triton burnt out, the PZT nanords will be crystallized into single crystal.

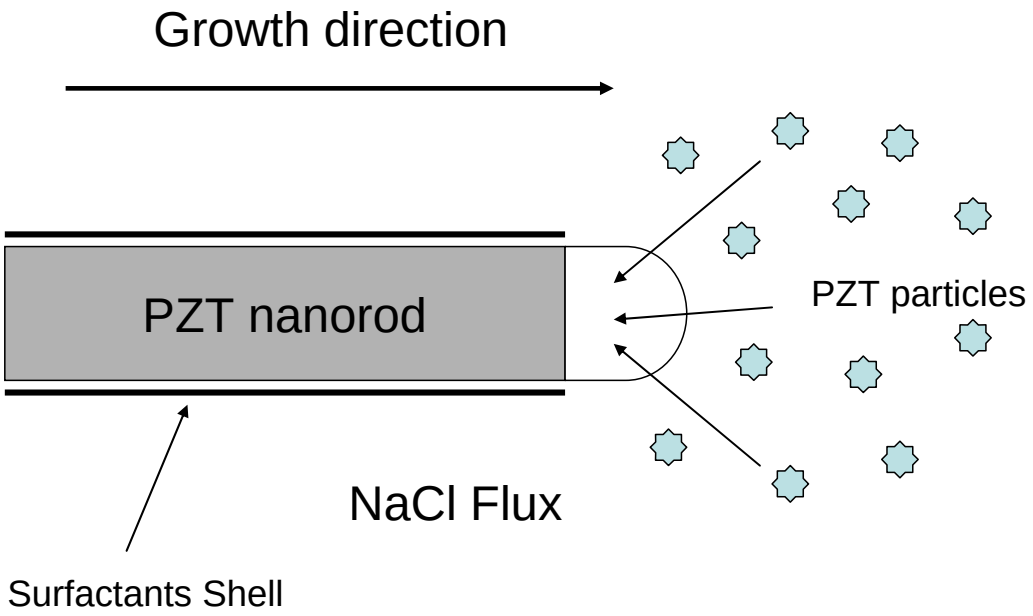

Figure 5.2 Proposed model of nanorod growth

5.3 Mechanism of PZT nanohexagon formation

The formation of PZT-nanohexagon in the mixture of Tween 20 and sodium chloride is related to Tween 20 chemical structure. Tween 20 (Polysorbate 20) is an

amphiphilic molecule with hydrophobic tail of hydrocarbon alkyl and hydrophilic tail of polyethylene glycol (PEG). The hydrophilic tail contains four branch chains of PEG. These PEGs will be stretched completely when surrounding temperature is high enough. The stretching angle between two PEG chains could be equal to the angle of hexagon. In the mixture of PZT nanocrystal, Tween 20 and sodium chloride, strong interactions exist between PEG and PZT nanocrystals. Therefore, PZT nanocrystals were adsorbed and located at the PEG parts of Tween 20, and grew into nanohexagon when temperature reaches 800°C. Figure 5.3 describes the hypothesis of the formation mechanism of PZT-nanohexagon.

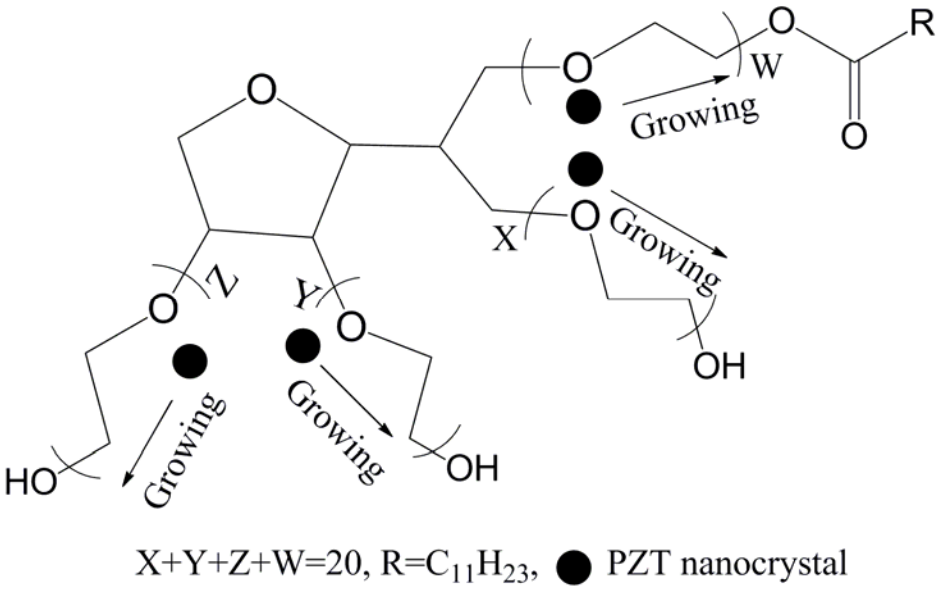

Figure 5.3 Mechanism of PZT nanohexagon formation.

Chapter 6 Conclusion

The sol-gel process is among the most extensively studied methods to fabricate PZT nanocrystals for microactuators and piezoelectric transducers. We have described the growth of single-crystalline PZT nanohexagons and nanorods using a surfactant-assisted sol-gel process. PZT nanocrystals were sintered with different duration and temperatures, and we discovered that PZT nanohexagons and nanorods were formed only at 800°C after 3 hours. Therefore, the growth of PZT nanohexagons and nanorods is very sensitive with the sintering time, temperature and surfactant we used. Single-crystalline PZT nanohexagons with diameters of about 480-540 nm and bounding lengths of approximately 230-260nm were synthesized when Tween 20 was used while single-crystalline PZT nanorods with diameters around 70-130 nm and lengths over 1 um were fabricated when Triton was used. The introducing of surfactant has been proved to be critical in the formation of single-crystalline PZT nanohexagons and PZT nanorods. The morphology and crystal structure of the PZT nanohexagons were characterized using X-ray diffraction, Raman Spectra, scanning electron microscopy and transmission electron microscopy. Our proposed process is a promising technique to produce single-crystalline PZT nanostructures.

Bibliography

[1] J. Johansson, J. Delsing. Microelectronics mounted on a piezoelectric transducer: Method, simulations, and measurements, Ultrasonics. 44 (2006) 1-11.

[2] G. Gautschi. Degree to disagree, INTECH. 49 (2002) 10-10.

[3] Harper, Douglas. "Piezoelectric". Online Etymology Dictionary.

[4] Holler, F. James; Skoog, Douglas A; Crouch, Stanley R (2007). "Chapter 1". Principles of Instrumental Analysis (6th ed.). Cengage Learning. p. 9. ISBN 9780495012016.

[5] http://en.wikipedia.org/wiki/Piezoelectricity

[6] S.S. Chandratreya, R.M. Fulrath, J.A. Pask. Reaction-Mechanisms in the Formation of Pzt Solid-Solutions, J Am Ceram Soc. 64 (1981) 422-425.

[7] W. COOK, H. JAFFE. The Crystallographic, Elastic, and Piezoelectric Properties of Ammonium Pentaborate and Potassium Pentaborate, Acta Crystallogr. 10 (1957) 705-707.

[8] S. VENKATARAMANI, J. BIGGERS. Densification in Pzt, Ferroelectrics. 37 (1981) 607-610.

[9] S. KIM, G. LEE, T. SHROUT, S. VENKATARAMANI. Fabrication of Fine-Grain Piezoelectric Ceramics using Reactive Calcination, J.Mater.Sci. 26 (1991) 4411-4415.

[10] N. Chakrabarti, H. Maiti. Chemical synthesis of PZT powder by auto-combustion of citrate-nitrate gel, Mater Lett. 30 (1997) 169-173.

[11] C. BRINKER, G. SCHERER. Sol-]Gel-]Glass .1. Gelation and Gel Structure,

J.Non Cryst.Solids. 70 (1985) 301-322.

[12] L. HENCH, J. WEST. The Sol-Gel Process, Chem.Rev. 90 (1990) 33-72.

[13] Klein, L. (1994). Sol-Gel Optics: Processing and Applications. Springer Verlag. ISBN 0792394240.

[14] G. ONODA, D. DOVE, L. HENCH. Analysis of Glass Container Coatings by Auger-Electron Spectroscopy, Am.Ceram.Soc.Bull. 52 (1973) 379-379.

[15] I. AKSAY, F. LANGE, B. DAVIS. Uniformity of Al2o3-Zro2 Composites by Colloidal Filtration Rid B-9281-2008, J Am Ceram Soc. 66 (1983) C190-C192.

[16] G. Franks, F. Lange. Plastic-to-brittle transition of saturated, alumina powder compacts, J Am Ceram Soc. 79 (1996) 3161-3168.

[17] A. EVANS, R. DAVIDGE. Strength and Fracture of Fully Dense Polycrystalline Magnesium Oxide, Philosophical Magazine. 20 (1969) 373-376.

[18] R. DAVIDGE, A. EVANS. Strength of Ceramics, Materials Science and Engineering. 6 (1970) 281-283.

[19] S. YAMAGISHI, Y. TAKAHASHI. Effect of Heating Atmosphere on Densification of Sol-Gel (Th, U)o-2 Microspheres, J.Nucl.Mater. 207 (1993) 255-265.

[20] F. LANGE, M. METCALF. Processing-Related Fracture Origins .2. Agglomerate Motion and Cracklike Internal Surfaces Caused by Differential Sintering, J Am Ceram Soc. 66 (1983) 398-406.

[21] A. EVANS. Considerations of Inhomogeneity Effects in Sintering, J Am Ceram Soc. 65 (1982) 497-501.

[22] Allman III, R.M., Structural Variations in Colloidal Crystals, M.S. Thesis,

UCLA (1983)

[23] Allman III, R.M. and Onoda, G.Y. (Unpublished work, IBM T.J. Watson Research Center, 1984.

[24] C. Galassi. Processing of porous ceramics: Piezoelectric materials RID C-3109-2009, J.Eur.Ceram.Soc. 26 (2006) 2951-2958.

[25] G. WHITESIDES, J. MATHIAS, C. SETO. Molecular Self-Assembly and Nanochemistry - a Chemical Strategy for the Synthesis of Nanostructures, Science. 254 (1991) 1312-1319.

[26] J. Aizenberg, A. Black, G. Whitesides. Control of crystal nucleation by patterned self-assembled monolayers, Nature. 398 (1999) 495-498.

[27] L. KLEIN, G. GARVEY. Kinetics of the Sol-Gel Transition, J.Non Cryst.Solids. 38-9 (1980) 45-50.

[28] C. BRINKER, K. KEEFER, D. SCHAEFER, C. ASHLEY. Sol-Gel Transition in Simple Silicates, J.Non Cryst.Solids. 48 (1982) 47-64.

[29] A. Einstein. A new determination of the molecular dimensions, Ann.Phys.-Berlin. 19 (1906) 289-306.

[30] S. SAKKA, K. KAMIYA. The Sol-Gel Transition in the Hydrolysis of Metal Alkoxides in Relation to the Formation of Glass-Fibers and Films, J.Non Cryst.Solids. 48 (1982) 31-46.

[31] PHILIPPO.W. Correlation of Elastic Properties in Steady-State Flow and Vibrational Experiments, J.Appl.Phys. 36 (1965) 3033-3036.

[32] E. Hauser, C. Reed. Studies in thixotropy I Development of a new method for measuring particle-size distribution in colloidal systems, J.Phys.Chem. 40 (1936)

1169-1182.

[33] M. Born. Thermodynamics of crystals and melting, J.Chem.Phys. 7 (1939) 591-603.

[34] M. Born. On the stability of crystal lattices. I, Proceedings of the Cambridge Philosophical Society. 36 (1940) 160-172.

[35] T. TANAKA. Collapse of Gels and Critical Endpoint, Phys.Rev.Lett. 40 (1978) 820-823.

[36] T. TANAKA. Gels, Sci.Am. 244 (1981) 124-127.

[37] T. TANAKA, L. HOCKER, G. BENEDEK. Spectrum of Light Scattered from a Viscoelastic Gel, J.Chem.Phys. 59 (1973) 5151-5159.

[38] T. TANAKA, D. FILLMORE, S. SUN, I. NISHIO, G. SWISLOW, A. SHAH. Phase-Transitions in Ionic Gels, Phys.Rev.Lett. 45 (1980) 1636-1639.

[39] J.D. Ferry, J.L. Oncley. Studies of the dielectric properties of protein solutions. III. Lactoglobulin. J.Am.Chem.Soc. 63 (1941) 272-278.

[40] J. Ferry. Studies of the mechanical properties of substances of high molecular weight I A photoelastic method for study of transverse vibrations in gels, Rev.Sci.Instrum. 12 (1941) 79-82.

[41] J. FERRY, E. FITZGERALD. Mechanical and Electrical Relaxation Distribution Functions of 2 Compositions of Polyvinyl Chloride and Dimethylthianthrene, J.Colloid Sci. 8 (1953) 224-242.

[42] H. BELTMAN, J. LYKLEMA. Rheological Monitoring of Formation of Polyvinyl Alcohol Congo Red Gels, Faraday Discuss. 57 (1975) 92-100.

[43] A. HECHT, E. GEISSLER. Dynamic Light-Scattering from

Polyacrylamide-Water Gels, Journal De Physique. 39 (1978) 631-638.

[44] E. GEISSLER, A. HECHT. The Poisson Ratio in Polymer Gels, Macromolecules. 13 (1980) 1276-1280.

[45] N. Sommerdijk, J. Wright. Matrix effects on selective chemical sensing by sol-gel entrapped complexing agents, J.Sol Gel Sci.Technol. 13 (1998) 565-568.

[46] S. Wallington, T. Labayen, A. Poppe, N. Sommerdijk, J. Wright. Sol-gel entrapped materials for optical sensing of solvents and metal ions, Sens.Actuator B-Chem. 38 (1997) 48-52.

[47] N. Sommerdijk, A. Poppe, C. Gibson, J. Wright. Unexpected complexation behaviour of a sol-gel immobilised dye: the development of an optical copper(II) sensor, J.Mater.Chem. 8 (1998) 565-567.

[48] N. Sommerdijk, E. vanEck, J. Wright. Highly defined pore size distribution in sol-gel silicate glasses induced by incorporation of an oligomeric siloxane, Chem.Commun. (1997) 159-160.

[49] C. BRINKER, G. SCHERER, E. ROTH. Sol-]Gel-]Glass .2. Physical and Structural Evolution during Constant Heating Rate Experiments, J.Non Cryst.Solids. 72 (1985) 345-368.

[50] C. BRINKER, E. ROTH, G. SCHERER, D. TALLANT. Structural Evolution during the Gel to Glass Conversion, J.Non Cryst.Solids. 71 (1985) 171-185.

[51] R. Gupta, N.K. Chaudhury. Entrapment of biomolecules in sol-gel matrix for applications in biosensors: Problems and future prospects, Biosens.Bioelectron. 22 (2007) 2387-2399.

[52] B. YOLDAS. Monolithic Glass-Formation by Chemical Polymerization,

J.Mater.Sci. 14 (1979) 1843-1849.

[53] S. PROCHAZKA, F. KLUG. Infrared-Transparent Mullite Ceramic, J Am Ceram Soc. 66 (1983) 874-880.

[54] P. Patel, G. Gilde, P. Dehmer, J. McCauley. Transparent ceramics for armor and EM window applications, Inorganic Optical Materials Ii. 4102 (2000) 1-14.

[55] C. Wang, J. Ying. Sol-gel synthesis and hydrothermal processing of anatase and rutile titania nanocrystals, Chem.Mat. 11 (1999) 3113-3120.

[56] D. Segal. Chemical synthesis of ceramic materials, J.Mater.Chem. 7 (1997) 1297-1305.

[57] H. Yin, Y. Wada, T. Kitamura, S. Kambe, S. Murasawa, H. Mori, et al. Hydrothermal synthesis of nanosized anatase and rutile TiO2 using amorphous phase TiO2, J.Mater.Chem. 11 (2001) 1694-1703.

[58] A. Schildknecht, R. Sauer, K. Thonke. Donor-related defect states in ZnO substrate material, Physica B. 340 (2003) 205-209.

[59] Y. Deng, L. Liu, Y. Cheng, C. Nan, S. Zhao. Hydrothennal synthesis and characterization of nanocrystalline PZT powders, Mater Lett. 57 (2003) 1675-1678.

[60] T. Morita. Piezoelectric Materials Synthesized by the Hydrothermal Method and Their Applications, MATERIALS. 3 (2010) 5236-5245

[61] T. Morita, Y. Wagatsuma, Y. Cho, H. Morioka, H. Funakubo, N. Setter. Ferroelectric properties of an epitaxial lead zirconate titanate thin film deposited by a hydrothermal method below the Curie temperature RID E-8484-2010, Appl.Phys.Lett. 84 (2004) 5094-5096.

[62] T. Morita, Y. Cho. A hydrothermally deposited epitaxial lead titanate thin film

on strontium ruthenium oxide bottom electrode RID E-8484-2010, Appl.Phys.Lett. 85 (2004) 2331-2333.

[63] T. Morita, Y. Cho. Piezoelectric property of an epitaxial lead titanate thin film deposited by the hydrothermal method RID E-8484-2010, Appl.Phys.Lett. 88 (2006) 112-118.

[64] K. SHIMOMURA, T. TSURUMI, Y. OHBA, M. DAIMON. Preparation of Lead Zirconate Titanate Thin-Film by Hydrothermal Method, Jpn.J.Appl.Phys.Part 1 - Regul.Pap.Short Notes Rev.Pap. 30 (1991) 2174-2177.

[65] K. MCAFEE, D. GAY, R. HOZACK, R. LAUDISE, G. SCHWARTZ, W. SUNDER. Thermodynamic Considerations in the Synthesis and Crystal-Growth of Gasb, J.Cryst.Growth. 76 (1986) 263-271.

[66] M. Kurosawa, S. Shimano, S. Ishii, K. Shima, T. Kato. Quantitative trace element analysis of single fluid inclusions by proton-induced X-ray emission (PIXE): Application to fluid inclusions in hydrothermal quartz, Geochim.Cosmochim.Acta. 67 (2003) 4337-4352.

[67] Spezzia, G. La Pressione e' Chimicamente Inattive Nella Solubilite e. Riecostituzione del Quarzo, Accad. Sci. Torino Atti 40 (1905) 254-262.

[68] R. LAUDISE, A. BALLMAN. Hydrothermal Synthesis of Sapphire, J.Am.Chem.Soc. 80 (1958) 2655-2657.

[69] K. KAKEGAWA, J. MOHRI, S. SHIRASAKI, K. TAKAHASHI. Sluggish Transition between Tetragonal and Rhombohedral Phases of Pb(zr,ti)o3 Prepared by Application of Electric-Field, J Am Ceram Soc. 65 (1982) 515-519.

[70] A. Shimojima, N. Umeda, K. Kuroda. Synthesis of layered inorganic-organic

nanocomposite films from mono-, di-, and trimethoxy(alkyl)silane-tetramethoxysilane systems, Chem.Mat. 13 (2001) 3610-3616.

[71] X. Cao, L. Xie, H. Zhan, Y. Zhou. Large-scale synthesis of Li(1.2)V(3)O(8) as a cathode material for lithium secondary battery via a soft chemistry route, Mater.Res.Bull. 44 (2009) 472-477.

[72] J. Nedelec, D. Avignant, R. Mahiou. Soft chemistry routes to YPO4-based phosphors: Dependence of textural and optical properties on synthesis pathways RID A-6920-2008, Chem.Mat. 14 (2002) 651-655.

[73] M.K. Ahmad, M. Rusop. Influence of Glacial Acetic Acid and Nitric Acid as a Chelating Agent in Sol-gel Process to the Nanostructured Titanium Dioxide Thin Films, Nanoscience and Nanotechnology. 1136 (2009) 339-344.

[74] G. YI, Z. WU, M. SAYER. Preparation of Pb(zr,ti)o3 Thin-Films by Sol-Gel Processing - Electrical, Optical, and Electro-Optic Properties Rid B-6408-2008, J.Appl.Phys. 64 (1988) 2717-2724.

[75] Y. TAKAHASHI, Y. MATSUOKA, K. YAMAGUCHI, M. MATSUKI, K. KOBAYASHI. Dip Coating of Pt, Pz and Pzt Films using an Alkoxide-Diethanolamine Method, J.Mater.Sci. 25 (1990) 3960-3964.

[76] S. DEY, K. BUDD, D. PAYNE. Thin-Film Ferroelectrics of Pzt by Sol-Gel Processing, IEEE Trans.Ultrason.Ferroelectr.Freq.Control. 35 (1988) 80-81.

[77] S. DEY, K. BUDD, D. PAYNE. Structure of Polymeric Pbtio3 Gels, J Am Ceram Soc. 70 (1987) C295-C296.

[78] P. Coffman, C. Barlingay, A. Gupta, S. Dey. Structure evolution in the

PbO-ZrO2-TiO2 sol-gel system .2. Pyrolysis of acid and base-catalyzed bulk and thin film gels, J.Sol Gel Sci.Technol. 6 (1996) 83-106.

[79] R. VEST, J. XU. Pbtio3 Films from Metalloorganic Precursors, IEEE Trans.Ultrason.Ferroelectr.Freq.Control. 35 (1988) 711-717.

[80] G. HAERTLING. Plzt Electrooptic Materials and Applications - a Review, Ferroelectrics. 75 (1987) 25-55.

[81] G. HAERTLING. Plzt Thin-Films Prepared from Acetate Precursors, Ferroelectrics. 116 (1991) 51-63.

[82] S. RAMAMURTHI, D. PAYNE. Structural Investigations of Prehydrolyzed Precursors used in the Sol-Gel Processing of Lead Titanate, J Am Ceram Soc. 73 (1990) 2547-2551.

[83] S. SENGUPTA, L. MA, D. ADLER, D. PAYNE. Extended X-Ray-Absorption Fine-Structure Determination of Local-Structure in Sol-Gel-Derived Lead Titanate, Lead Zirconate, and Lead-Zirconate-Titanate, J.Mater.Res. 10 (1995) 1345-1348.

[84] C. LAKEMAN, Z. XU, D. PAYNE. On the Evolution of Structure and Composition in Sol-Gel-Derived Lead-Zirconate-Titanate Thin-Layers, J.Mater.Res. 10 (1995) 2042-2051.

[85] B. Guiffard, M. Troccaz. Low temperature synthesis of stoichiometric and homogeneous lead zirconate titanate powder by oxalate and hydroxide coprecipitation, Mater.Res.Bull. 33 (1998) 1759-1768.

[86] C. Law, K. Tong, J. Li, K. Li. Effect of pyrolysis temperature on the characteristics of PZT films deposited by the sol-gel method, Thin Solid Films. 335

(1998) 220-224.

[87] J. Frantti, V. Lantto, S. Nishio, M. Kakihana. Effect of A- and B-cation substitutions on the phase stability of PbTiO3 ceramics, Phys.Rev.B. 59 (1999) 12-15.

[88] J. Frantti, V. Lantto. Structural studies of Nd-modified lead zirconate titanate ceramics between 11 and 680 K at the morphotropic phase boundary, Phys.Rev.B. 56 (1997) 221-236.

[89] C. Bae, H. Yoo, S. Kim, K. Lee, J. Kim, M.A. Sung, et al. Template-directed synthesis of oxide nanotubes: Fabrication, characterization, and applications RID A-6791-2010 RID A-2388-2010 RID D-5107-2009, Chem.Mat. 20 (2008) 756-767.

[90] G. Cao, D. Liu. Template-based synthesis of nanorod, nanowire, and nanotube arrays RID E-4799-2011, Adv.Colloid Interface Sci. 136 (2008) 45-64.

[91] S. Limmer, S. Seraji, M. Forbess, Y. Wu, T. Chou, C. Nguyen, et al. Electrophoretic growth of lead zirconate titanate nanorods RID B-3717-2012 RID E-4799-2011, Adv Mater. 13 (2001) 1269-1272.

[92] Y. Lin, G. Wu, X. Yuan, T. Xie, L. Zhang. Fabrication and optical properties of TiO2 nanowire arrays made by sol-gel electrophoresis deposition into anodic alumina membranes, J.Phys.-Condes.Matter. 15 (2003) 2917-2922.

[93] Y. Luo, I. Szafraniak, N. Zakharov, V. Nagarajan, M. Steinhart, R. Wehrspohn, et al. Nanoshell tubes of ferroelectric lead zirconate titanate and barium titanate RID B-4159-2012 RID B-7811-2011 RID B-9197-2011, Appl.Phys.Lett. 83 (2003) 440-442.

[94] Y. Luo, I. Szafraniak, V. Nagarajan, R. Wehrspohn, M. Steinhart, J. Wendorff, et al. Ferroelectric lead zirconate titanate and barium titanate nanotubes RID B-4159-2012 RID B-9197-2011 RID B-7811-2011, Integrated Ferroelectr. 59 (2003) 1513-1520.

[95] X. Zhang, X. Zhao, C. Lai, J. Wang, X. Tang, J. Dai. Synthesis and piezoresponse of highly ordered Pb(Zr0.53Ti0.47)O-3 nanowire arrays, Appl.Phys.Lett. 85 (2004) 4190-4192.

[96] Y. Wang, J. Santiago-Aviles. Synthesis of lead zirconate titanate nanofibres and the Fourier-transform infrared characterization of their metallo-organic decomposition process, Nanotechnology. 15 (2004) 32-36.

[97] H. Liang, S. Liu, S. Yu. Controlled Synthesis of One-Dimensional Inorganic Nanostructures Using Pre-Existing One-Dimensional Nanostructures as Templates RID B-7292-2011 RID A-1903-2010, Adv Mater. 22 (2010) 3925-3937.

[98] X. Peng, L. Manna, W. Yang, J. Wickham, E. Scher, A. Kadavanich, et al. Shape control of CdSe nanocrystals RID G-2339-2010, Nature. 404 (2000) 59-61.

[99] G. Xu, Z. Ren, P. Du, W. Weng, G. Shen, G. Han. Polymer-assisted hydrothermal synthesis of single-crystalline tetragonal perovskite PbZr0.52Ti0.48O3 nanowires, Adv Mater. 17 (2005) 907-1001.

[100] Y. Xia, P. Yang, Y. Sun, Y. Wu, B. Mayers, B. Gates, et al. One-dimensional nanostructures: Synthesis, characterization, and applications RID E-8499-2011 RID A-3683-2010 RID A-3949-2011 RID D-5987-2011, Adv Mater. 15 (2003) 353-389.

[101] Z.L. Wang. Oxide nanobelts and nanowires - Growth, properties and

applications RID E-2176-2011, J.Nanosci.Nanotechnol. 8 (2008) 27-55.

[102] M. Law, J. Goldberger, P. Yang. Semiconductor nanowires and nanotubes RID F-5484-2011, Ann.Rev.Mater.Res. 34 (2004) 83-122.

[103] B.A. Wacaser, K.A. Dick, J. Johansson, M.T. Borgstrom, K. Deppert, L. Samuelson. Preferential Interface Nucleation: An Expansion of the VLS Growth Mechanism for Nanowires RID A-2497-2009 RID A-8579-2008 RID B-6433-2008 RID B-2237-2008 RID A-6719-2008 RID A-2171-2010, Adv Mater. 21 (2009) 153-165.

[104] Wagner, R. S.; Albert P. Levitt (1975). Whisker Technology. Wiley – Interscience – New York. ISBN 0-4715-3150-2.

[105] Nic, M.; Jirat, J.; Kosata, B., eds. (2006). "Ostwald ripening". IUPAC Compendium of Chemical Terminology (Online ed.). doi:10.1351/goldbook.O04348. ISBN 0-9678550-9-8.

[106] W. Ostwald. **1896**. Lehrbuch der Allgemeinen Chemie, vol. 2, part 1. Leipzig, Germany.

[107] Ratke, Lorenz; Voorhees, Peter W. (2002). Growth and Coarsening: Ostwald Ripening in Material Processing. Springer. pp. 117–118. ISBN 3540425632.

[108] Hubbard, Arthur T. (2004). Encyclopedia of Surface and Colloid Science. CRC Press. p. 4230. ISBN 0824707591.

[109] M. Niederberger, H. Coelfen. Oriented attachment and mesocrystals: Non-classical crystallization mechanisms based on nanoparticle assembly RID A-6144-2008, Phys.Chem.Chem.Phys. 8 (2006) 3271-3287.

[110] K. Yoon, Y. Cho, D. Kang. Molten salt synthesis of lead-based relaxors,

J.Mater.Sci. 33 (1998) 2977-2984.

[111] R. Walton. Subcritical solvothermal synthesis of condensed inorganic materials RID C-2058-2009, Chem.Soc.Rev. 31 (2002) 230-238.

[112] John Roach (2007-02-13). ""No Two Snowflakes the Same" Likely True, Research Reveals". National Geographic News. http://news.nationalgeographic.com/news/2007/02/070213-snowflake.html. Retrieved 2009-07-14.

[113] R. Song, H. Coelfen. Mesocrystals-Ordered Nanoparticle Superstructures, Adv Mater. 22 (2010) 1301-1330.

[114] R. Penn. Kinetics of oriented aggregation, J Phys Chem B. 108 (2004) 12707-12712.

[115] K. Taguchi, J. Garside, N. Tavare. Nucleation and growth kinetics of barium sulphate in batch precipitation, J.Cryst.Growth. 163 (1996) 318-328.

[116] A. CHIANESE, F. DIBERARDINO, A. JONES. On the Effect of Secondary Nucleation on the Crystal Size Distribution from a Seeded Batch Crystallizer Rid C-1805-2008, Chem.Eng.Sci. 48 (1993) 551-560.

[117] P. Caron, High gamma ' solvus new generation nickel-based superalloys for single crystal turbine blade applications, MINERALS, METALS & MATERIALS SOC, WARRENDALE; 184 THORN HILL RD, WARRENDALE, PA 15086-7514 USA, 2000.

[118] Y.C. Cho, S. Lee, M. Ajmal, W. Kim, C.R. Cho, S. Jeong, et al. Copper Better than Silver: Electrical Resistivity of the Grain-Free Single-Crystal Copper Wire, Cryst.Growth Des. 10 (2010) 2780-2784.

[119] R. Thomas, S. Mochizuki, T. Mihara, T. Ishida. Preparation of ferroelectric Pb(Zr-0.5,Ti-0.5)O-3 thin films by sol-gel process: dielectric and ferroelectric properties, Mater Lett. 57 (2003) 2007-2014.

[120] N. Dharmaraj, C. Kim, H. Kim. Pb(Zr-0.5, Ti-0.5)O-3 nanofibres by electrospinning, Mater Lett. 59 (2005) 3085-3089.

[121] N.J. Phillips, S.J. Milne, N.J. Ali, J.D. Kennedy. A preliminary nuclear-magnetic-resonance investigation of the titanium Diisorpropoxide Bis(2,4-Pentanedionate) Propanediol sol-gel precursor system, J. Mater. Sci. Lett. 13 (1994) 1535-1537.

[122] W. Wang, C. Xu, G. Wang, Y. Liu, C. Zheng. Preparation of Smooth Single-. Crystal Mn3O4 Nanowires, Adv. Mater. 14 (2002) 837-840.

[123] P. W. Vorhees, Annu. Ostwald ripening of two phase mixtures, Rev. Mater. Sci. 22 (1992) 197-215.

[124] Y. Chen, J. Li, Q. Wei, H. Zhai. Preparation and growth mechanism of TaCx whiskers RID D-3931-2011, J.Cryst.Growth. 224 (2001) 244-250.